NANO · MICRO small
www.small-journal.com

Periodic Flows in Microfluidics

Amith Mudugamuwa, Uditha Roshan, Samith Hettiarachchi, Haotian Cha, Hafiz Musharaf, Xiaoyue Kang, Quang Thang Trinh, Huan Ming Xia, Nam-Trung Nguyen, and Jun Zhang**

Microfluidics, the science and technology of manipulating fluids in microscale channels, offers numerous advantages, such as low energy consumption, compact device size, precise control, fast reaction, and enhanced portability. These benefits have led to applications in biomedical assays, disease diagnostics, drug discovery, neuroscience, and so on. Fluid flow within microfluidic channels is typically in the laminar flow region, which is characterized by low Reynolds numbers but brings the challenge of efficient mixing of fluids. Periodic flows are time-dependent fluid flows, featuring repetitive patterns that can significantly improve fluid mixing and extend the effective length of microchannels for submicron and nanoparticle manipulation. Besides, periodic flow is crucial in organ-on-a-chip (OoC) for accurately modeling physiological processes, advancing disease understanding, drug development, and personalized medicine. Various techniques for generating periodic flows have been reported, including syringe pumps, peristalsis, and actuation based on electric, magnetic, acoustic, mechanical, pneumatic, and fluidic forces, yet comprehensive reviews on this topic remain limited. This paper aims to provide a comprehensive review of periodic flows in microfluidics, from fundamental mechanisms to generation techniques and applications. The challenges and future perspectives are also discussed to exploit the potential of periodic flows in microfluidics.

1. Introduction

Microfluidics is the science and technology of manipulating minute volumes of fluids in channels ranging from several microns to several hundreds of microns.[1] This field offers numerous advantages, including low energy consumption,[2] minimal material and fluid usage,[3,4] precise control,[5] fast reaction,[6] high throughput,[7] integration of multiple functions,[8] process optimization and automation,[9] multiplexing,[10] and increased portability.[11,12] As a result, microfluidics has found applications in a wide range of fields, such as biomedical assays,[13] particle manipulation,[14] on-chip diagnostics,[15] genetic engineering,[16] and neuroscience.[17] Additionally, microfluidic systems can mimic biological functions, leading to the development of organ-on-a-chip (OoC) devices that replicate human organ functions.[18,19]

Fluid dynamics within microchannels greatly affect the functionality of microfluidic devices. In microfluidics, fluid flow typically is at low Reynolds numbers, where viscous forces dominate over inertial forces, resulting in laminar flow.[20] Mixing in laminar regimes is limited by molecular diffusion.[21] Periodic flows, such as pulsatile and oscillatory flows, are characterized by cyclic patterns over time. When properly designed, these flows can enhance the functionality, performance, and adaptability of microfluidic devices in biomedicine, chemistry, and engineering.[22] For instance, pulsations can induce flow instabilities that improve fluid mixing in low Reynolds number flows.[23,24] Oscillatory flows can also extend the effective length of microchannels, which is beneficial for submicron and nanoparticle manipulation by inertial and viscoelastic forces.[25,26] Mimicking human biological functions in microfluidics using periodic flow can facilitate the understanding of disease mechanisms, drug development, and personalized medicine.[27] Emerging OoC approaches aim to recapitulate pulsation features of cardiovascular to study cellular behaviors and interactions related to cardiovascular physiology, pathology, and pharmacology.[28]

To date, many periodic flow generation techniques have been reported, including syringe pumps,[29] peristalsis,[30] pneumatic,[31,32] electric,[33] magnetic,[34,35] acoustic,[36,37] mechanical,[38] and fluidic actuation,[39,40] as well as methods

A. Mudugamuwa, U. Roshan, S. Hettiarachchi, H. Cha, H. Musharaf, X. Kang, Q. T. Trinh, N.-T. Nguyen, J. Zhang
Queensland Micro and Nanotechnology Centre
Griffith University
Brisbane, QLD 4111, Australia
E-mail: nam-trung.nguyen@griffith.edu.au; jun.zhang@griffith.edu.au
H. M. Xia
School of Mechanical Engineering
Nanjing University of Science and Technology
Nanjing 210094, P. R. China
J. Zhang
School of Engineering and Built Environment
Griffith University
Brisbane, QLD 4111, Australia

The ORCID identification number(s) for the author(s) of this article can be found under https://doi.org/10.1002/smll.202404685

DOI: 10.1002/smll.202404685

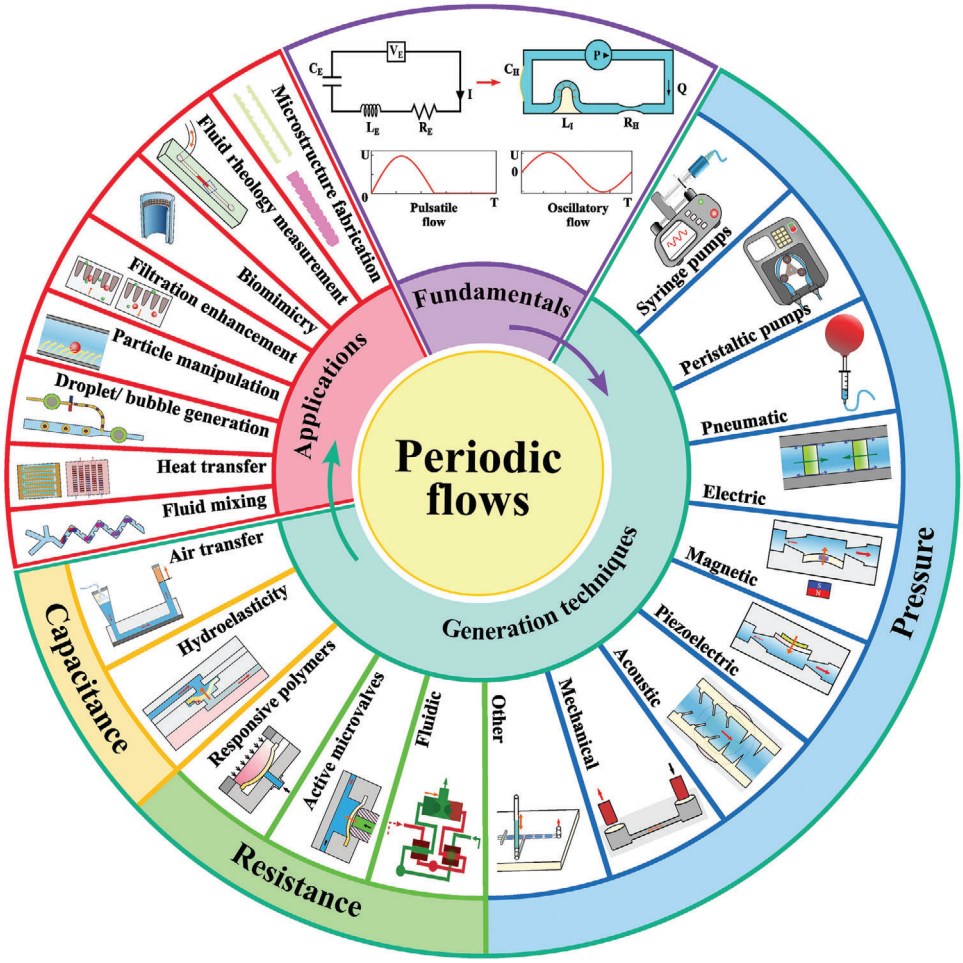

Figure 1. A schematic overview of periodic flows in microfluidics, covering theoretical fundamentals, generation techniques, and applications.

using material phase transitions,[41,42] hydroelasticity,[43,44] and air bubble flexibility.[45] Despite the significant importance of the versatile and efficient generation of periodic flows, comprehensive reviews on this topic are scarce. So far, only one paper has reviewed the pulsatile flow in microfluidics, with a particular focus on applications.[46] Periodic flow generation is vital for microfluidic systems. Understanding and controlling these flows are essential for designing efficient and reliable microfluidic systems.

This review aims to provide a comprehensive overview of periodic flows in microfluidics, including the fundamentals of periodic flows, generation techniques, and their applications as illustrated in **Figure 1**. We first explain the theoretical fundamentals of periodic flows using the hydraulic-electric analogy. Next, we study the working principles, device designs, and performances of periodic flow generation techniques based on the classification of pressure, resistance, and capacitance. Furthermore, we summarize the recent advances in applications of periodic flow in fluid mixing, heat transfer, droplet/bubble generation, particle manipulation, filtration enhancement, biomimicry etc. Finally, we discuss the challenges and future research directions in harnessing the potential of periodic flows.

2. Fundamentals of Periodic Flows in Microfluidics

2.1. Pulsatile and Oscillatory Flows

Fluid flows in microchannels can be steady or unsteady (**Figure 2**). Steady flows indicate that the fluid velocity is constant and independent of time everywhere in the microchannels (Figure 2A). In contrast, fluid velocity varies with time in magnitude, direction, or both in unsteady flows. Periodic flows are a type of unsteady flow, and the fluid motion in microchannels exhibits repetitive patterns over time. The two most common periodic flows are pulsatile and oscillatory flows.[47]

In a pulsatile flow, the fluid has a net movement after a period (Figure 2B). For example, heart pumping in the human cardiovascular system generates a rhythmic pulsatile blood flow throughout the body.[50] Pulsatile flows induce fluctuating shear stresses on the walls of the channel or vessel, significantly affecting the behavior of suspended particles, cells, or biological tissues.[46,51,52] Therefore, the pulsatile flows are ubiquitous in cleaning fouling deposits in bio-industrial equipment,[47] mitigating filter clogging,[53] automating bioassays,[54] and improving cell cultures.[55]

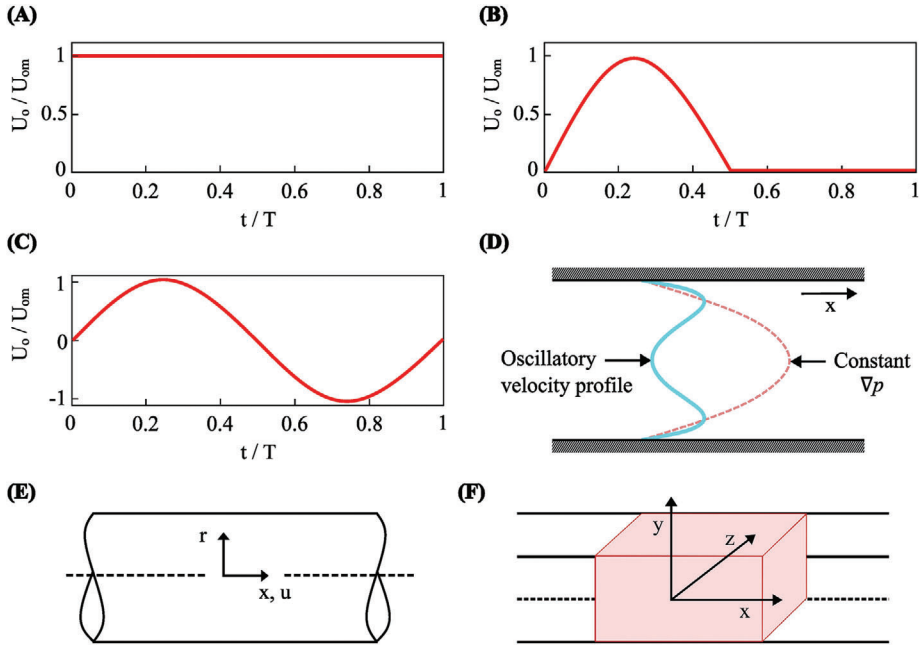

Figure 2. The flow velocity profile of A) steady flow, B) simple pulsatile flow, and C) an oscillatory flow profile where U_o/U_{om} is the ratio of instantaneous velocity to the maximum velocity. Reproduced with permission.[46] Copyright 2019, John Wiley and Sons. D) Velocity profile under steady and periodic Poisuelle flows. Reproduced with permission.[48] Copyright 2012, Springer Nature. Reproduced with permission.[49] Copyright 2010, The Institute of Physics. E) Circular microchannel and coordinates. F) Rectangular microchannel and coordinates.

Oscillatory flows share some similarities with pulsatile flows but are typically distinguished by periodic back-and-forth motion rather than pulsations in flow velocity.[56] Figure 2C shows oscillatory flows with a net-zero flow rate of each cycle. These net-zero flow properties can create virtually "infinite" long channels, where fluid and suspended particles can be transported with sufficient residual time, which is especially advantageous for the lateral migration of small particles.[26,57] The waveforms of oscillatory flows can be sinusoidal, square, triangular, and sawtooth.[58]

2.2. Oscillatory Reynolds Number (Re_o)

In steady flows, Reynolds number (Re), defined as the ratio between inertial forces and viscous forces, can be used to predict fluid flow regimes.[59–61] In oscillatory flow, the oscillatory Reynolds number (Re_o), derived based on Re and oscillation characteristics, has been used to determine the nature of an oscillatory fluid flow.

$$Re = \frac{Inertial\ forces}{Viscous\ forces} = \frac{u\, d_h}{\nu} = \frac{\rho\, u\, d_h}{\mu} \tag{1}$$

$$Re_o = \frac{2\,\pi\, f\, x_0\, \rho\, d_h}{\mu} \tag{2}$$

Here, ρ is the fluid density, d_h is the channel hydraulic diameter, μ is the dynamic viscosity, ν is the kinematic viscosity, u is the (time-independent) mean flow velocity, f is the oscillation frequency, and x_o is the amplitude.

2.3. Governing Equations for Oscillatory Flow

The incompressible Navier-Stokes equation considering uniform-viscous Newtonian fluids with no body forces is given by the Equation (3), where $\vec{u}$ is the fluid velocity field, t is time, and p is the pressure.[62–64]

$$\rho \frac{\partial \vec{u}}{\partial t} = -\rho\, \vec{u}\, \nabla\, \vec{u} - \nabla p + \mu\, \nabla^2\, \vec{u} \tag{3}$$

The governing equation for a time-dependent fluid flow in a straight channel is:[63–65]

Considering a pressure-driven oscillatory laminar flow (see Figure 2D),[48,49] characterized by zero mean velocity in a straight microchannel with circular or rectangular cross sections, the Navier-Stokes equation can be written as:[65–68]

$$\frac{\partial \vec{u}}{\partial t} = K \cos \omega t + \nu\, \nabla^2\, \vec{u} \tag{4}$$

Here, K is the magnitude of the oscillations, and ω is the frequency. $\nabla 2$ is expressed as $(\frac{\partial^2}{\partial x^2} + \frac{1}{r}\frac{\partial}{\partial r}(r\frac{\partial}{\partial r}))$ in circular microchannels (Figure 2E), and equals to $(\frac{\partial^2}{\partial y^2} + \frac{\partial^2}{\partial z^2})$ for rectangular microchannels (Figure 2F).

2.4. Hydraulic-Electric Analogy

The fluid transport in microfluidics shares a similar law with the electrical current transport in electrical circuits. For example, the parameter given by Hagen-Poiseuille's law for fluidic resistance is analogous to the electric resistance given by

Table 1. The analogy between fluidic and electric circuits.[62,70,72–76]

Fluidics	Electronics
Volume V [m^3]	Electric charge q [C]
Flow rate Q [$m^3\ s^{-1}$]:	Current I [A]:
Pressure P [$N\ m^{-2}$]:	Voltage V_E [V]:
Fluidic resistance R_H [$N\ s\ m^{-5}$]: $\Delta P = Q R_H$	Electric resistance R_E [Ω]: $V_E = I R_E$
Fluidic inertia (hydraulic inertance) L_I [$kg\ m^{-4}$]: $L_I = \rho \frac{l}{A} = \frac{\Delta P}{(d(Q)/dt)}$	Inductance L_E [H]: $L_E = \frac{\Phi_{(I)}}{I} = \frac{V_E}{(d(I)/dt)}$
Fluidic capacitance C_H [$m^5\ N^{-1}$]: $Q = C_H \frac{d(P)}{dt} + P \frac{d(C_H)}{dt}$	Electric capacitance C_E [F]: $I = C_E \frac{d(V_E)}{dt} + V_E \frac{d(C_E)}{dt}$

Ohm's law in an electronic circuit.[62,69] Further details of this hydraulic-electric analogy are summarized in **Table 1** and illustrated in **Figure 3**.[70,71] In the equations, t is the time, ρ is the fluid density, l is the microchannel length, A is the channel cross sectional area, and $\Phi_{(I)}$ is the magnetic flux of current I. This analogy helps to analyze sophisticated fluidic behaviors and design complex channel networks.

2.4.1. P-R_H Circuit

For a fluidic circuit that consists of a pressure source (P) and a fluidic resistance $R_{H,}$ based on Hagen-Poiseuille's law, the volumetric flow rate of fluids within the channel is:[69]

$$Q = \frac{\Delta P}{R_H} \tag{5}$$

Equation (5) shows that periodic flow rates can be obtained by varying the pressure difference (ΔP) across the channel, the fluidic resistance (R_H), or both. Many on-chip and off-chip pumps have been reported to provide time-dependent pressure sources for driving fluid flow.[77,78]

The fluidic resistance (R_H) is a function of channel geometry, dimensions, and fluidic properties. The fluidic resistances of a straight microchannel with circular (R_{cir}) and rectangular (R_{rec}) cross sections are respectively expressed as:[79]

$$R_{cir} = \frac{8\,\mu\,l}{\pi\,r_i^4} \tag{6}$$

$$R_{rec} \approx \frac{12\,\mu\,l}{w\,h^3\left(1 - \frac{0.63\,h}{w}\right)} \tag{7}$$

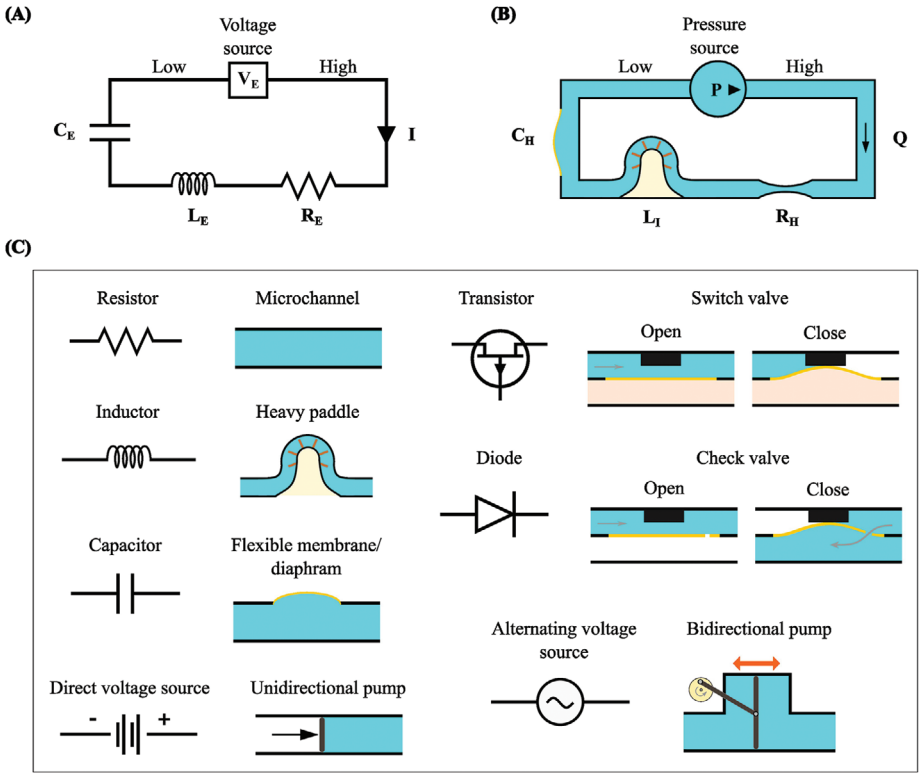

Figure 3. The schematic of the hydraulic-electric analogy. Reproduced with permission.[70] Copyright 2023, The Royal Society of Chemistry. A) Typical electrical circuit. B) Fluidic circuit. C) Electrical components and respective analogous fluidic elements.

where r_i is the channel radius, w is the channel width, and h is the channel height. Equation (7) assumes that w is greater than h. Externally controlling the channel dimensions, e.g., shrinking the cross sectional area to a minimum and creating substantial fluidic resistance, can switch off the fluid flow, also called fluidic transistors.[70,80]

2.4.2. P-R_H-C_H Circuit

Well-tuned fluidic resistance and capacitance can generate and drive desired flows in microfluidics over constant pressure sources.[81] A compliant element (i.e., an elastic or compressible structure) can provide both fluidic resistance and capacitance.[82] Deformation of a compliant element changes the dimensions of the microchannel or microchamber and, hence, the fluidic resistance in the microfluidic network.[83] This can be used to dynamically regulate the fluid flow. In addition, a compliant capacitive element can store potential energy by changing its shape or size. In flow stabilizers, capacitive elements are carefully designed to reduce undesired pulsations in the microfluidic network.[84–86] Besides, capacitive elements can induce pulsations in the fluid flow using active or passive methods.[43,44,87]

This capacitive element can be an elastic membrane in a microchamber, and its capacitance depends on its shape and thickness.[70] If the membrane and the microchamber are circular, the capacitance (C_{cir}) is:

$$C_{\underset{\text{membrane}}{\text{cir}}} = \frac{\pi\, r^6 \left(1-\sigma^2\right)}{16\, E\, \delta^3} \tag{8}$$

where r is the membrane radius, σ is Poisson's ratio, E is Young's modulus, and δ is the thickness of the membrane.

For a rectangular capacitor, its capacitance (C_{rec}) is expressed as:[70]

$$C_{\underset{\text{membrane}}{\text{rec}}} = \frac{3\, a^4\, \left(1-\sigma^2\right)}{\pi\, E\, \delta^3}\, \frac{a\, b}{3+2\, n^2+3\, n^4},\ n=\frac{a}{b} \tag{9}$$

Here, a and b are the length and width of the rectangular membrane, respectively.

In addition to elastomeric membranes, air bubbles,[88] compressible fluid,[89] and elastic tubing[90] are also capacitive components in microfluidic systems. The hydrodynamic capacitance of an elastic tube (C_{tube}) was found to have a damping effect on hydrodynamic fluctuations in microfluidic systems and is expressed as:[91]

$$C_{\text{tube}} = \frac{2\,\pi\, r_i^2\, l\, \left[(1+\sigma)\, r_o^2-(1-2\,\sigma)\, r_i^2\right]}{E\, \left(r_o^2-r_i^2\right)} \tag{10}$$

where r_i is the inner diameter, r_o is the outer diameter of the tube.

For microfluidic devices made of compressible materials, e.g., polydimethylsiloxane (PDMS), microchannels can deform to adapt to fluid pressure, which increases or decreases the channel volume. The capacitance of such a rectangular microchannel can be estimated as:[92]

$$C_{\underset{\text{microchannel}}{\text{rec}}} = \frac{\alpha\, h\, w\, l\, (1+\sigma)}{E} \tag{11}$$

where α is a constant coefficient depending on the ratio w/h.

Based on the above discussion, we can conclude that time-dependent periodic flows can be obtained by controlling the driven pressure and fluidic resistance in real time or employing fluidic capacitive components to induce oscillatory flows. In the next chapter, we will elaborate on the existing techniques for generating periodic flows from these three fundamental aspects.

3. Periodic Flow Generation

Various off-chip or on-chip, active or passive methods can generate periodic flow in microfluidic channels. The off-chip methods use separated equipment to produce the pressure source and control fluid flow.[93] These devices are connected to the microfluidic device by fluidic tubing. Therefore, the adverse effects of off-chip devices (e.g., mechanical vibrations) minimally affect the microfluidic arrangement.[94] However, these systems are bulky.[95] Conversely, on-chip actuators are incorporated into the microfluidic chip to control fluid flow in microchannels. These actuators can increase the portability of microfluidic systems by reducing the size and power requirement.[96] Actuation can be active, using external force fields such as mechanical, chemical, electrical,[97–104] or passive, relying on forces such as capillary, viscous, and gravitational.[55,105–112] The fundamental theory discussed above leads to three strategies for generating periodic flows: driven pressure, fluidic resistance, or capacitance. This section will elaborate on the current development of periodic flow generation techniques from these three aspects and explain the generation mechanism, device design, performance, pros and cons.

3.1. Pressure

The most common technique for generating periodic flows is directly varying the driven pressure for the microfluidic system.[113] This section discusses various techniques and devices that can produce variable pressure sources (**Figure 4A**).

3.1.1. Syringe Pumps

Syringe pumps are the most conventional devices in microfluidics due to the simplicity of setting up and operating (Figure 4B).[117,118] These are infusion-type pumps with a syringe that exerts force to control fluid flow rate.[119] The force is either applied manually or using a motor.[120,121] The pump performance is impacted by the syringe size[122] and the compliance of the tubing between the pump and the device.[123–125] In terms of generating a periodic flow, the speed of the piston movement can be varied as necessary.[126] The flow rate of a motorized syringe pump is controlled by modulating the supply voltage of the direct current (DC) motor. Commercial laboratory syringe pumps are supplied by Harvard Apparatus, Postnova Analytics GmbH, Landgraf Laborsysteme HLL GmbH, Longer Precision Pump Co. Ltd., New Era Instruments, Masterflex, DK Infusetek Co. Ltd., etc.

Common syringe pumps operate in open-loop; thus, the real-time flow rate cannot be determined while using this equipment.

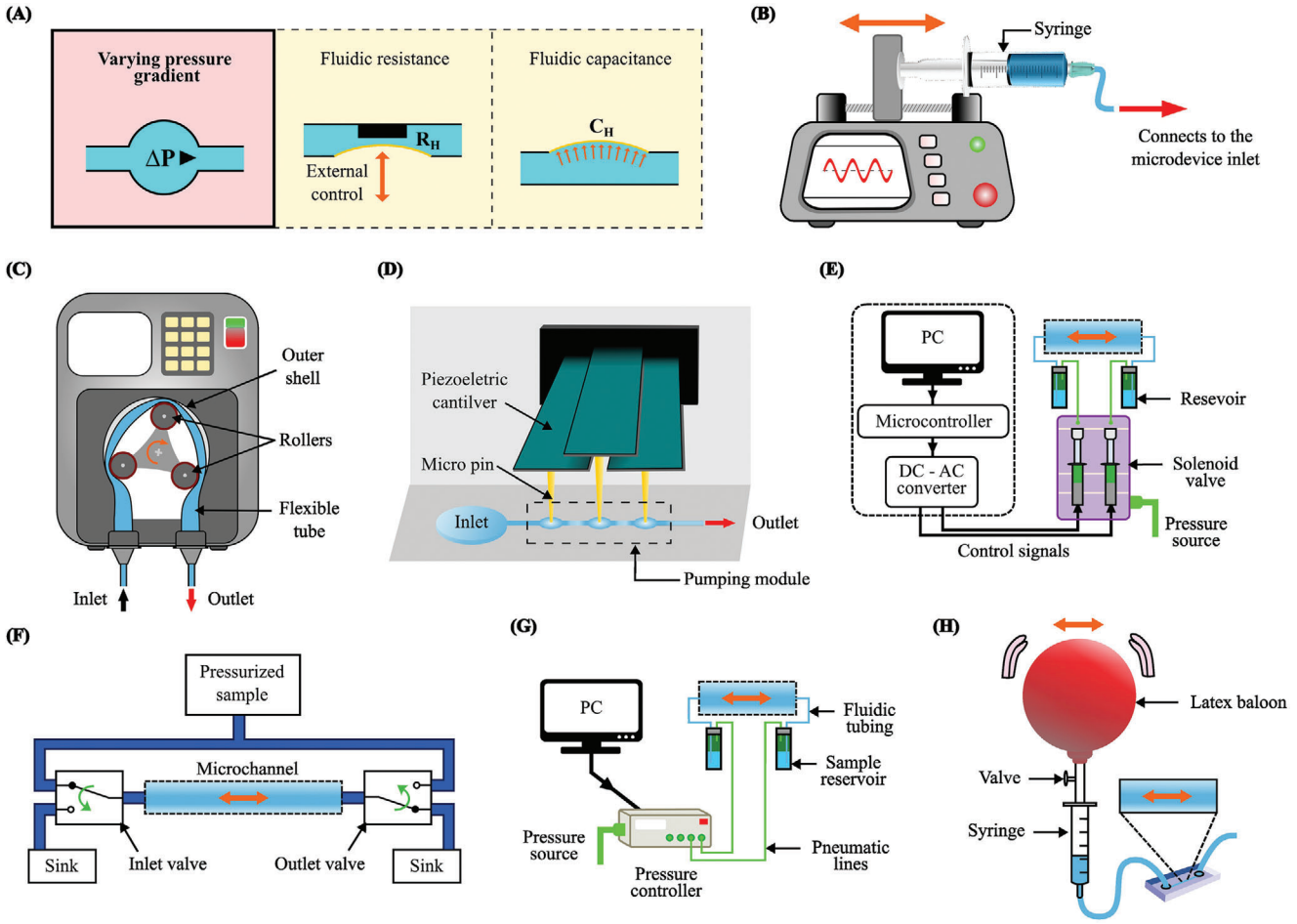

Figure 4. A) Pressure-based periodic flow generation. B) Single-piston syringe pump. Reproduced with permission.[114] Copyright 2023, The Public Library of Science. C) Conventional roller-type peristaltic pump. Reproduced with permission.[115] Copyright 2023, Frontiers. D) Peristaltic micropump with flexible membranes actuated sequentially using piezoelectric micro pins. Reproduced with permission.[30] Copyright 2019, Elsevier. E) Periodic actuation of solenoid valves to control pneumatic pressure supply. Reproduced with permission.[25] Copyright 2020, The American Chemical Society. F) Use of two 3-way valves at the inlet and outlet to generate forward and reverse flow. Reproduced with permission.[116] Copyright 2019, Springer Nature. G) Regulating pneumatic pressure using an electronic pressure controller. Reproduced with permission.[53] Copyright 2022, The Royal Society of Chemistry. H) Squeezing and releasing a latex balloon can generate periodic pressure. Reproduced with permission.[93] Copyright 2018, The Royal Society of Chemistry.

The mean flow rate of a motorized syringe pump can be accurate, but the flow profile can be noisy due to the mechanical vibrations induced by the motor.[127] The size of syringe pumps is large compared to the size of the microfluidic chips, negatively affecting their portability.[128] Syringe pumps with feedback using proportional-integral (PI) and proportional-integral-derivative (PID) control techniques can increase the linearity of the flow profile.[129] The fluid volume that can be pumped using a syringe pump is limited.[130] Therefore, syringe pumps are incompatible with applications requiring continuous fluid flow over a long period or when fluid recirculation is required. However, programmable syringe pumps with infusing and withdrawing features can generate periodic flows.[131] Programmable syringe pumps often generate oscillatory flows with low frequency ($0.1\ \text{Hz} \leq f \leq 10\ \text{Hz}$).[31] In addition to directly controlling the fluid flow with a single programmable syringe pump at the inlet, two or more pumps can also be configured to operate simultaneously.[127] For example, in a two-syringe pump setup, the primary pump continuously produced the bulk flow, while the secondary pump produced pulsations with pre-configured infusing and withdrawal functions.[29] The produced periodic flow meets the bulk flow at a T-junction, and the resultant flow becomes periodic.

3.1.2. Peristaltic Pumps

Peristalsis is the natural phenomenon of contraction and relaxation of muscles involuntarily to push fluids, primarily in the digestive tract.[132] Devices that use peristalsis motion to produce a fluid flow are called peristaltic pumps.[133] The peristaltic roller pump comprises a motorized rotating roller that compresses and releases a flexible tube periodically.[105] The flow rate of a peristaltic pump depends on this compressing and releasing

frequency.[134] The outer shell accommodates the flexible tube, and the roller is designed to trap a small fluid volume inside the flexible tube and pull along with the rotational movement of the roller.[135] This motion produces a pressure gradient inside the tube, generating fluid flow.[136] Peristaltic roller pumps are bidirectional (Figure 4C), so they are suitable for producing periodic flows.[137] Furthermore, these are extremely useful when unidirectional, pulsatile, and oscillatory flows must be generated using the same hardware configuration.[138] Several leading suppliers of peristaltic roller pumps include Leadfluid, Shenchen Baoding Precision Pump Co. Ltd, Vapourtec Ltd., Longer Precision Pump Co. Ltd., ISMATEC, New Era Instruments, and Dolomite Microfluidics.

Peristaltic pumps are tagged as contact-free devices because their components do not directly contact the fluid inside the flexible tube.[137] Additionally, they are preferred in applications requiring continuous fluid flow or recirculation.[139] Multi-channel peristaltic pumps can deliver fluid for multiple inlets.[140,141] A significant limitation of peristaltic pumps is the undesired pulsatile flow caused by periodic compression of the tube or channel.[119] This negatively affects applications requiring steady and pulseless flow. Peristaltic pumps without rotating rollers have been studied to mitigate long-term tubing damage due to the outer surface shear forces.[142–145] Peristaltic pumps are commonly expensive and large and have significantly fewer customization features.[146]

Miniaturization of peristaltic pumps in microfluidics has also been reported.[147–150] Commonly, peristaltic micropumps consist of three microchambers with a flexible membrane on the top or bottom wall. These three membranes are sequentially actuated by an external force to generate the desired flow.[151–153] For example, three piezoelectric cantilevers deformed the flexible membrane with micro pins (Figure 4D).[30,154] Programming the piezoelectric micropin actuators can vary the flow direction. In addition, peristaltic micropumps can be actuated using pneumatic, electrostatic, magnetic, mechanical, electrochemical, and thermal methods.[155–158] Parameters such as the operating frequency, stroke volume, and actuation sequence are significant when using peristaltic micropumps to generate periodic flows.[156] Peristaltic micropumps have advantages, such as resistance to high backpressure, tolerance to unnecessary bubble formation, endurance, and self-priming.[159]

3.1.3. Pneumatic Actuation

Pneumatic-based systems are widely used in microfluidics due to their higher degree of controllability. In pneumatic systems, compressed air is supplied using a pressure source and guided to a sealed reservoir connected to the inlet of microfluidic devices.[160] Compressors and pressure pumps are commonly used as the pressure source in pneumatic pumping systems. In pneumatic-based systems (Figure 4E), flow regulation is achieved by partially or entirely closing valves.[25] Electromechanical valves, controlled by periodic waveforms from a signal generator, can regulate the flow rate and direction.[31] A simple periodic flow generation setup connects a positive and a negative pressure source to a solenoid valve.[32] Cyclic opening and closing of the solenoid valve generate the periodic flow. Changing the opening and closing time of the valve creates a range of frequencies. Asghari et al.[25] generated an oscillatory flow using a single pressure source and two solenoid valves. A computer, microcontroller, and a DC to alternating current (AC) converter produced the AC control signal, operating the solenoid valves. In addition, high-speed 3-way valves connected to a single pressure source can generate periodic flows.[161] A configuration consisting of a valve at the inlet and another at the outlet of a microfluidic channel was used to create an oscillatory flow (Figure 4F).[26] The periodic signal supplied to the inlet valve was inversed to control the valve at the other end of the channel.[116]

Electronic (or digital) pressure controllers have been widely used to regulate pressure in microfluidic systems (Figure 4G).[162] The flow rate magnitude and direction in these devices can be electronically altered.[31] Mutlu et al. utilized an electronic pressure controller with a 3-way valve to generate periodic flows.[163] In this study, the electronic pressure controller maintains the constant pressure at the two inlets, where the 3-way valve generates the pulsations. A net forward flow is achieved by slightly reducing the outlet pressure or setting a shorter "ON" time for reverse flow than the forward flow. Besides, each channel of an electronic pressure controller can be separately controlled. To generate an oscillatory flow using a single channel, a pressure source and a vacuum source to operate on both positive and negative parts of the pressure signal are required. The very low response time (≈10 ms for 100 mbar) of these devices is an advantage for flow regulation. However, differences between the target and actual output waveforms must be considered for higher frequencies and amplitudes.[50] Elveflow OB1-MK3 and Fluigent Flow-EZ are electronic pressure controllers in the market specially designed for microfluidics.

A latex balloon connected to a microfluidic system via a syringe containing the working fluid can also generate a periodic flow (Figure 4H).[164] Flow rate variations are induced by iteratively squeezing and releasing the balloon either manually or automatically.[93] The suitability of reinforced latex balloons (using elastane fibers) has been demonstrated for high-flow rate applications.[165] The thickness, number of layers, and circumference of the balloon affect the flow rate. Latex balloon-based pumping is self-sufficient, contact-free with the working fluid, low-cost, accessible, simple, and portable. However, latex balloon-based systems are less accurate and have a limited fluid volume.

3.1.4. Electric Actuation

Electric fields can effectively deliver fluid using electrokinetic mechanisms such as electroosmosis and electrothermal effects.[100,166] Transporting an electrolyte solution through a microchannel or a porous material upon applying an electric field refers to electroosmosis.[167] The interaction of the electrolyte solution and the solid surface forms an electric double layer between the fluid and the charged surface. The applied electric field interacts with the electric double layer and exerts a force on the ions in the diffuse layer to move them. Therefore, an electroosmotic flow can be simply generated by applying a voltage between the two ends of a microchannel without the use of mechanical parts.[168] Electroosmotic transportation is common for

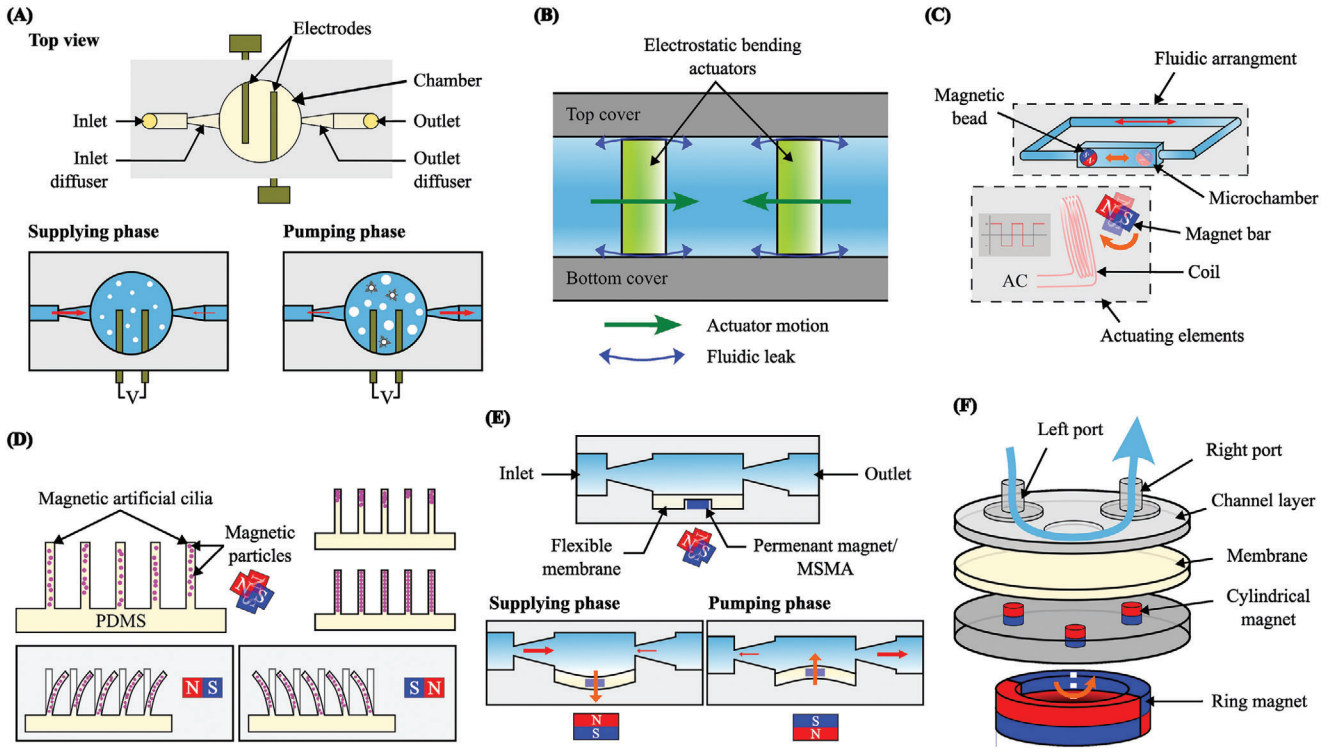

Figure 5. A) Electrolysis generates nanobubbles to regulate the fluid flow. Reproduced with permission.[33] Copyright 2016, The Institute of Physics. B) Electrostatically bending actuators to squeeze fluid toward the outlet. Reproduced with permission.[178] Copyright 2018, MDPI. C) Oscillating a magnetic bead using a rotating magnet. Reproduced with permission.[78] Copyright 2021, John Wiley and Sons. D) Controlling magnetic artificial cilia using a permanent magnet to regulate the fluid flow. Reproduced with permission.[34] Copyright 2018, Elsevier. E) Moving a MSMA element or a permanent magnet embedded in a flexible membrane can obtain periodic pumping. Reproduced with permission.[35] Copyright 2020, Elsevier. Reproduced with permission.[41] Copyright 2023, Springer Nature. F) Peristaltic motion using a rotating ring-type permanent magnet. Reproduced with permission.[179] Copyright 2022, MDPI.

lower-conductive fluids because increasing conductivity can significantly decrease flow velocity.[169,170]

A unidirectional flow can be generated by imposing a DC voltage, whereas an AC electric field can produce an oscillatory flow. For example, an AC electric field imposed on a microchannel with a solution of electric conductivity of 200 μS cm^{-1} generated a flow that alternated between the two reservoirs relative to the AC signal.[57] For the working fluid with a high electric conductivity, electro-thermal effects are significant to induce a fluid flow.[100] In electrothermal actuation, electric heating produces temperature gradients and induces body forces to move the fluid inside the microchannel.[171] The amount of heat generation depends on the fluid conductivity and the applied electric field. Discretized electrodes have successfully generated bidirectional flows using a medium with an electrical conductivity from 0.1 to 1 Sm^{-1}.[172] However, regulating the fluid flow using Joule heating significantly limits the pulsating frequency.[173,174]

Similarly, electrolysis can control fluid flows in microfluidic devices.[175] When water serves as the electrolyte and a voltage is applied on metallic electrodes, H_2 and O_2 bubbles are formed.[33] These bubbles acquired space inside the microchamber, pushing the working fluid outwards (**Figure 5A**). Integrating a nozzle/diffuser maintains a net forward fluid flow while generating a pulsatile flow. The divergence angle, nozzle length, neck width, and chamber depth are important parameters.[176] Electrostatic bending actuators drive fluids in microfluidic devices using the nano electrostatic driving principle, which combines electrostatic forces with the bimorph leverage.[177] Two actuators were sandwiched between silicon layers and actuated in opposite directions, squeezing and expanding the working fluid (Figure 5B).[178] Due to passive valves, the forward flow is higher than the backward flow, generating a pulsatile flow upon electrostatic actuation.

3.1.5. Magnetic Actuation

Magnetically actuated particles or structures have been used to generate periodic flows.[149,150] Oscillating a magnetic bead inside a microchamber affected the fluid flow inside (Figure 5C).[78] The bead was oscillated using a rotating magnet. Depending on the structure of the microchamber, the generated flow can be unidirectional or bidirectional. The magnetic bead is not easy to wear because it moves freely inside the chamber. This concept eliminates interference from the current, electric field, or chemical activity and is highly resistant to blockage due to debris. Besides, the magnetic bead can be electromagnetically controlled using an audio signal from a computer or a mobile device.

Artificial cilia mimic biological cilia, hair-like structures used for transportation by synchronized movements.[180] Zhang et al.

developed an array of magnetic artificial cilia using a composite of silicone elastomer (PDMS) and magnetic microparticles (Carbonyl iron powder) (Figure 5D).[34] This array can be externally controlled using a permanent magnet or electromagnet. Magnetic actuation can generate oscillatory and pulsatile flows. Artificial cilia respond instantaneously to the external magnetic actuation and can achieve flow rates up to 250 μL s^{-1}. Shape memory alloys are smart materials capable of memorizing geometries,[181,182] and they can respond to stimuli such as heat, light, solvents, electricity, magnetic fields, pH changes, etc.[183] Magnetic shape memory alloys (MSMA) can change their geometry depending on the intensity of the magnetic field and the polarity. Saren et al.[41] used this phenomenon with Ni-Mn-Ga alloy element in a micropump with a nozzle/diffuser structure (Figure 5E). Rotating a permanent magnet by a DC motor generated a periodic magnetic field that could operate the MSMA element. The generated flow was pulsatile, and an oscillatory flow was achieved by alternatively changing the rotating direction of the DC motor.

Similarly, an elastic membrane coupled with a permanent magnet can dynamically deform under a periodically varying magnetic field.[35,184] Peristaltic motion can also be generated by sequential deformation of elastic membranes within three chambers (Figure 5F).[179,185] The membrane was deformed at three locations by the movements of permanent magnets actuated by a custom-made ring-type magnet. When the ring-type magnet was rotated, the membrane in each chamber was systematically expanded or retracted. Therefore, a periodic flow was induced, and this device has further been used to perform oscillatory flow polymerase chain reaction (PCR).

3.1.6. Piezoelectric Actuation

Piezoelectric materials (e.g., lead zirconate titanate, lithium niobate, lithium tantalate, and quartz) generate mechanical vibrations using electricity and vice versa.[186,187] Piezoelectric elements are widely used to regulate microchamber volume for generating fluid flows.[188] A typical micropump shown in **Figure 6A**, consists of a chamber with a diaphragm attached to a piezoelectric element and a nozzle or diffuser structure on the two sides of the chamber. By actuating the piezoelectric element, the diaphragm is deflected to squeeze the fluids inside. Periodic deflection produces a volumetric change in the chamber, generating the alternating pressure difference to suck in and discharge the fluid.[189] The nozzle/diffuser structures maintain a positive net flow.[190] Maximum flow rates up to 150 μL min^{-1} and 512 μL s^{-1} were reported using piezoelectric transducers.[190,191] In these micropumps, the backward flow is inevitably present, resulting in a pulsatile fluid flow.

A piezoelectrically actuated glass membrane performed on-chip pumping with a resolution of 1.4 nL.[200] An oscillatory flow was generated using two similar on-chip pumps oriented in opposite directions. In addition, microvalves were used to regulate flows in microfluidic devices.[192,201] In the work of Dong et al., a check valve was opened in the suction stroke and closed in the compression stroke, allowing the fluid to flow unidirectionally toward the outlet.[201] This ultimately generated a pulsatile flow, resulting in a maximum pumping flow rate of 33.91 mL s^{-1}. More recently, ferroelectric nanocomposites have been used to optimize the performance of flexible membranes.[202] The supplying voltage significantly decreased from 1000 to 160 V, and a broad flow rate from 0.78 to 8.1 mL s^{-1} was achieved.

3.1.7. Acoustic Actuation

Acoustic waves can manipulate fluid flow and particles, and the combination of acoustics and microfluidics is called acoustofluidics.[203–205] In general, acoustic waves are divided into surface acoustic waves (SAWs) and bulk acoustic waves (BAWs). In SAWs, the vibration only propagates on the surface, but in BAWs, the entire body vibrates.[206] SAWs are produced by integrating interdigitated transducers (IDTs), and localized fluid-substrate interactions induce acoustic streaming (Figure 6B). An acoustofluidic pump was developed using a C-shaped IDT within a triangle-edged microchannel.[193] The generated local streaming could produce a stable unidirectional flow at a rate of approximately nanoliters per second, with precise digital control and a response time of ≈1 s.

Sharp-edge-structures-based devices and acoustic bubbles-based devices can also generate periodic flows using BAWs.[207] Sharp-edge-structures-based devices consist of sharp microscale structures on channel walls (Figure 6C).[36] When these microstructures are oscillated, acoustic streaming is induced, generating a periodic flow in the microchannel. Pumping and mixing using sharp-edge structures with different shapes and orientations was reported.[194] Bachman et al.[194] generated acoustic waves using a cell phone and a portable speaker. This setup eliminated conventional bulky equipment such as function generators and signal amplifiers. This setup also offered a complete portable testing platform with a maximum flow rate of 99.83 nLs^{-1}, which is comparatively higher than a conventional setup.

Similarly, acoustic oscillations of bubbles produce acoustic streaming due to the non-linear effect caused by inertial and viscous forces.[37] Gao et al.[195] reported a microstructure arrangement with small and large microbubbles in opposite directions to achieve bi-directional flow control (Figure 6D). The resonant frequencies of the small and large bubbles were 24 Hz and 19 Hz, respectively. Therefore, the flow direction changes instantly when the supplied frequency is changed between the two operating frequencies. The maximum flow rate achieved was 26.66 nL s^{-1}. Bubble-based acoustofluidic devices are simple to fabricate and operate. However, the performance is affected by bubble instability, temperature dependence, and inconvenience of the bubble-trapping process.[36]

Harmonic mechanical movements of connecting tubings can generate periodic flows. Acoustic signals can be converted to mechanical motion. In a study, sound waves generated with a commercially available speaker were used to produce axial pulses in the inlet tube of the microfluidic setup (Figure 6E).[196] Transferring this axial vibration into the fluid flow generates dynamic flow patterns. Therefore, simply supplying harmonic sound waves to the speaker using a smartphone induces periodic flows. This highly controllable technique can be implemented without changing the device geometry. Besides, Vishwanathan et al.[31] investigated the inertial focusing and microscale mixing in oscillatory flows, which were generated by connecting a

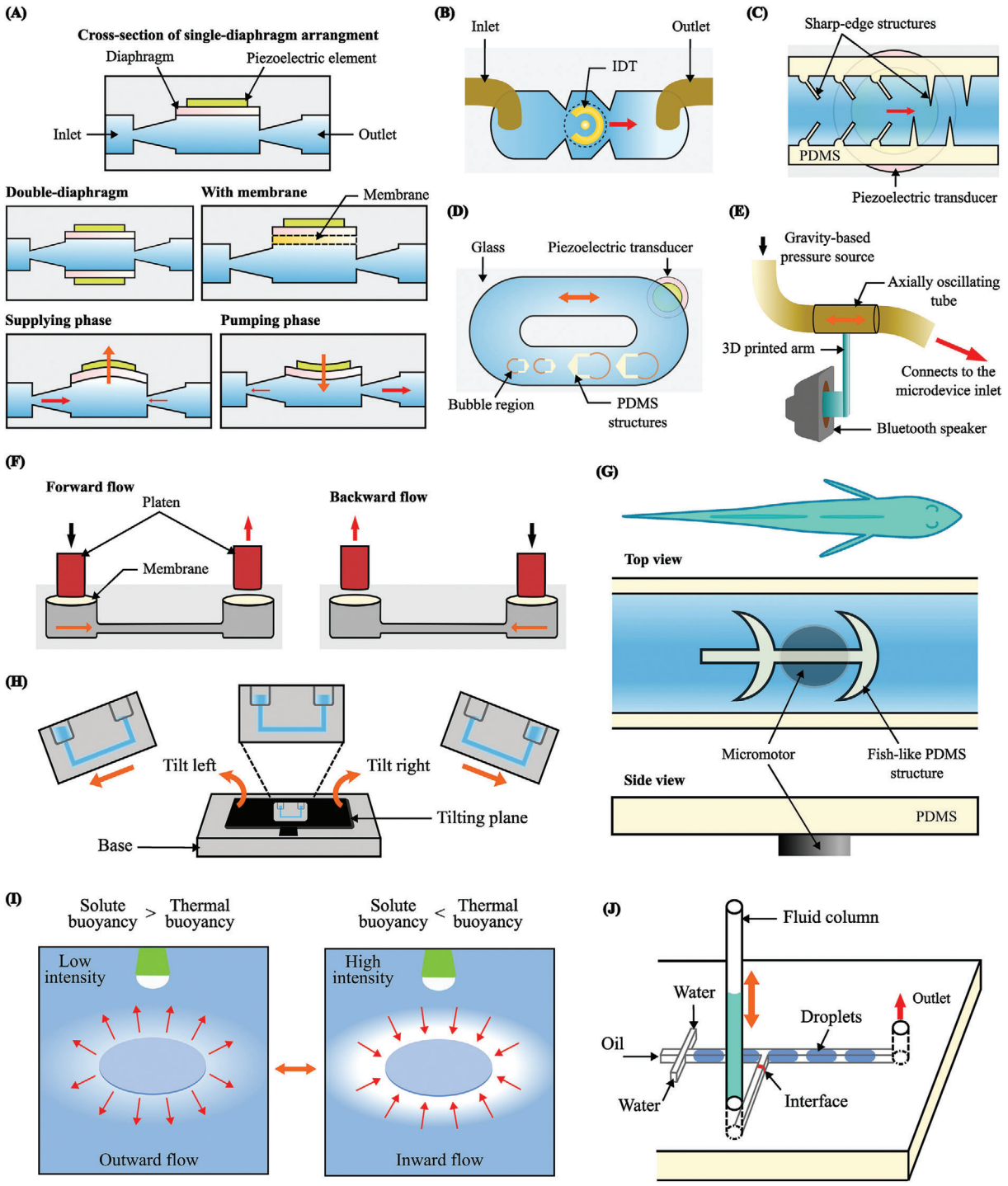

Figure 6. A) Piezoelectric actuation using a single-flexible diaphragm or double-diaphragm embedded in an elastic membrane. Reproduced with permission.[192] Copyright 2019, MDPI. B) IDT-based acoustic streaming produces a periodic fluid flow. Reproduced with permission.[193] Copyright 2019, The American Chemical Society. C) Sharpe-edge-structures-based acoustic streaming. Reproduced with permission.[194] Copyright 2018, The Royal Society of Chemistry. D) Bubble-based bidirectional flow control using related resonance frequencies. Reproduced with permission.[195] Copyright 2020, Springer Nature. E) Axial vibration-induced dynamic flow control. Reproduced with permission.[196] Copyright 2021, The Royal Society of Chemistry. F) Deforming flexible membranes using bipolar stepper motors. Reproduced with permission.[38] Copyright 2023, Springer Nature. G) Vibrating a fish-like microstructure using a micromotor creates a pulsatile flow with net forward flow. Reproduced with permission.[197] Copyright 2019, The American Institute of Physics. H) The tilting plane or rocker platform generates oscillatory flow using gravitational force. Reproduced with permission.[198] Copyright 2021, John Wiley and Sons. I) Light-powered micropump modulates fluid flow direction based on illumination intensity. Reproduced with permission.[104] Copyright 2018, Springer Nature. J) A stream of droplets travelling in a microchannel creates a periodic pressure drop in a perpendicular channel. Reproduced with permission.[199] Copyright 2019, Springer Nature.

loudspeaker diaphragm directly to the inlet tubing of the microfluidic device.

3.1.8. Mechanical Actuation

The mechanical motion of motors has been used to manipulate flows in microfluidic devices.[208] Truesdell et al.[38] used a pair of linear actuators controlled by two bipolar stepper motors to compress PDMS membranes (Figure 6F). The flexible membranes on the top of the fluid reservoirs at both ends of a straight microchannel were alternatively compressed. Compression and retraction of the reservoir walls using the 3D-printed actuators generated an oscillatory flow. However, the stepper motors significantly increased the size of the device. Another method to create pulsatile flows is to use a fish-like micropaddle structure vibrated by a micromotor (Figure 6G).[197] This device obtained a maximum net flow rate of 2.13 mL s^{-1}. A lab-on-a-chip (LoC) was realized using multiple vibrating micropaddles to perform analysis, sensing, and reacting functions. These micropaddles can be actuated by piezoelectric, electrostatic, electromagnetic, or shape memory alloy methods.

3.1.9. Other Concepts

Gravity-driven systems use the potential energy of the fluid (i.e., hydrostatic pressure) for actuation.[209] The gravitational force drives the fluid downstream, converting potential energy to kinetic energy, (Figure 6H). Therefore, gravity-driven systems are a passive pumping method in microfluidics. These methods are low-cost and do not encounter air trapping due to buoyancy.[210] However, gravity-driven systems require the reservoir to be placed at a considerable height to achieve higher flow rates. Placing a microfluidic device on a tilting plane (or a rocker platform) can generate periodic flows.[211] When two reservoirs at the inlet and outlet of a microdevice are alternatively tilted to change their relative height, the height difference creates a fluctuating pressure difference due to the gravitational force.[198,211]

Light-sensitive materials have been used as actuators to manipulate flows in microfluidics. Li et al.[104] developed a device 300 µm in size using perovskite and poly[(2-methoxy-5-ethylhexyloxy)−1,4-phenylenevinylene] (MEHPPV) and demonstrated successful directional control enabling the generation of periodic flows (Figure 6I). Illuminating the device with a 2 mm light spot resulted in four pumping stages: outward pumping, no pumping, heartbeat-like pumping, and inward pumping at 0.08, 0.45, 1, and 1.2 W cm^{-2} light intensities, respectively. The photo-degradation process of perovskite material increases the solution density near the pancake-like structure and drives the fluid outward at very low light irradiation, which is defined as the solute buoyancy mechanism.[212] At very high illumination, inward pumping is observed. This is because perovskite and MEHPPV absorb light and convert it to thermal energy, causing thermal buoyancy.[213] At medium light intensity, the micropump stops due to the balance of these two phenomena. Therefore, cyclic flow patterns were generated by modulating light intensities from low (0.08, 0.14, and 0.45 W cm^{-2}) to high (1.1 and 1.2 W cm^{-2}). Specifically, a heartbeat-like pumping was generated at an intensity ranging from 0.65 to 1.05 W cm^{-2} with frequency from 0.3 to 1.3 Hz, respectively.

Another interesting technique is utilizing a continuous stream of droplets and a perpendicular channel, in which a fluid-fluid interface is connected to a fluid column (Figure 6J).[199] A stream of droplets can be generated using cross-flow, flow-focusing, or co-flow channel geometries.[214] The pressure difference at the T-junction causes the fluid-fluid interface to oscillate at the perpendicular channel. The droplet length and width, viscosities of continuous and dispersed phases, droplet velocity, and the interfacial tension affect the pressure drop.

3.2. Fluidic Resistance and Fluidic Transistor

Fluidic resistance exists when a fluid flows through a microchannel. The magnitude of fluidic resistance depends on the geometry parameters of the microchannels and the fluid viscosity. Equations (5–7) indicate that the fluid flow rate can be controlled by adjusting the fluidic resistance, which can be easily achieved by deforming the microchannels using an external force (**Figure 7A**). Therefore, a periodic flow can be induced by harmonically varying the fluidic resistance in a microchannel. The fluid flow controlled by external forces is similar to electronic transistors.

In electronics, transistors are significant due to their ability to transfer an electric charge upon reaching a threshold voltage, which leads to decision-making. This provides the foundation for logical data processing in electronic circuits.[39] When the fluid flow in a microchannel is controlled by deflecting a flexible structure using the fluid pressure from the nearby microchannels or microchambers, the device works as a fluidic transistor to open or close the flow as well as to control the flow rate.[217,218] In digital signal processing, oscillator and digital logic capabilities are significant; however, amplification, regulation, and level-shifting functions are required in analogue signal processing.[219–221] The ability to perform these functions using fluidic transistors opens new research fields in on-chip fluidic signal processing.[42,80,222,223]

Fluidic oscillators are an excellent example of the application of fluidic transistors in digital flow control.[39] These oscillators use internal fluid dynamics to provide autonomous flow switching. Fluidic oscillators can convert a constant fluid flow to a periodic flow without additional actuation elements or dynamic controllers. Elastomeric membranes integrated into microchambers are commonly used to regulate flows in these oscillators. The configuration of the microchannel network and the geometry of microchambers are critical for the pulsatile flow function of fluidic transistors. A fluidic oscillator depicted in Figure 7B, has a pair of 4-terminal switch valves to create the oscillation and two check valves to stop the backflow.[39] Each switch valve has two terminals as the inlet and outlet for the green fluid and similarly, two terminals for the red fluid. Two fluids drive in separate microchannels in two layers, with a membrane separating the layers. The pressure difference in these two microchannels deforms the membrane inward or outward. This provides

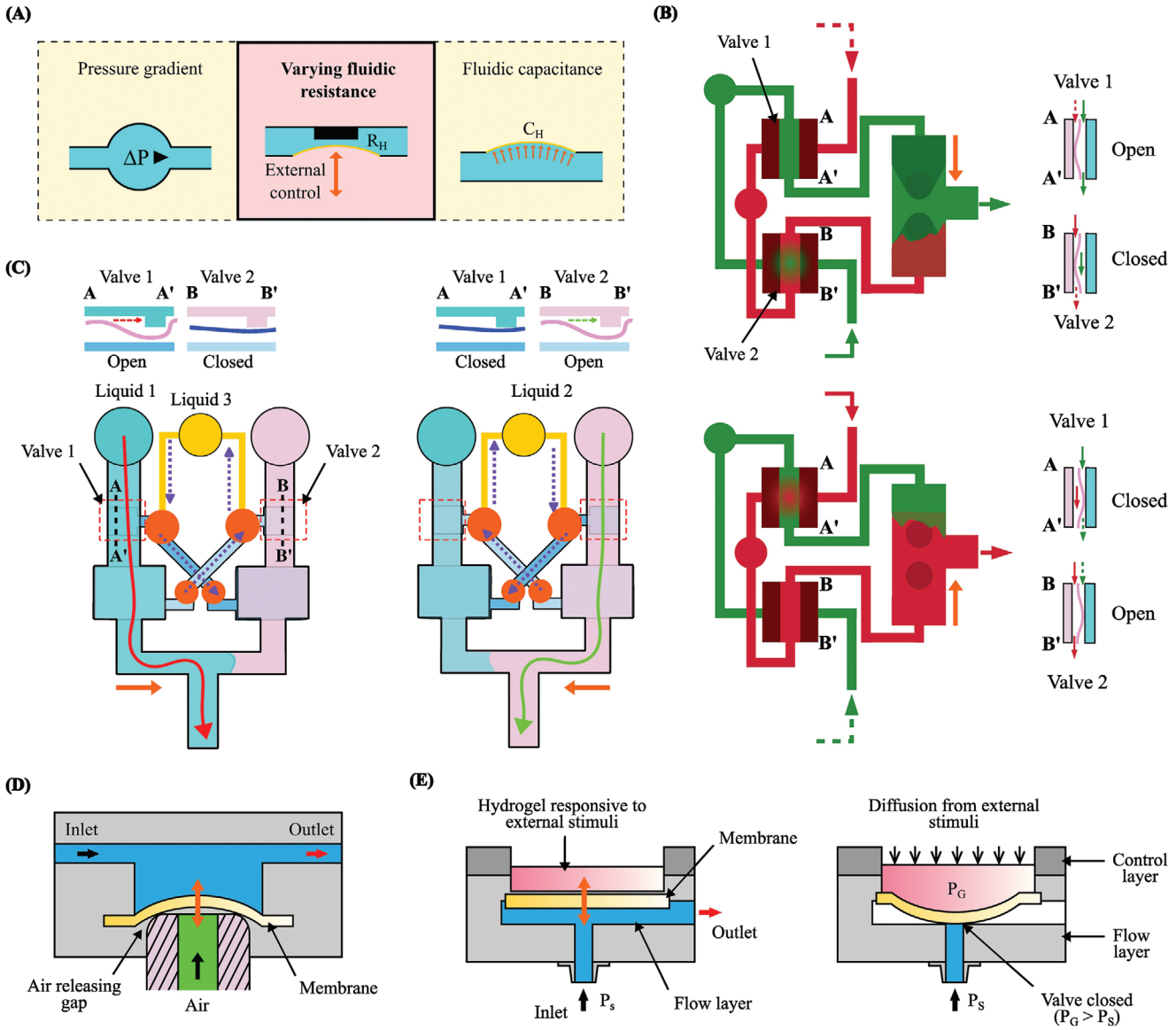

Figure 7. A) Fluidic resistance (transistor)-based periodic flow generation. B) Autonomous flow switch with 4-terminal valves using constant flows at inlets. Reproduced with permission.[39] Copyright 2010, Springer Nature. C) Water-head driven fluidic oscillator using 3-terminal valves. Reproduced with permission.[215] Copyright 2017, The Royal Society of Chemistry. Microvalve functionality using D) pneumatic-actuated deformation of a flexible membrane; Reproduced with permission.[216] Copyright 2013, The Royal Society of Chemistry. and E) expansion-retraction of phase transition hydrogels. Reproduced with permission.[42] Copyright 2016, The Public Library of Science.

the functionality of a switch valve, allowing only one type of fluid to pass through at a given instance. The green fluid passes through when 'valve 1' is open until pressure from the red fluid on the membrane increases and deforms toward the green fluid channel, closing the path for the green fluid. Then, the red fluid begins flowing through 'valve 2'. 'Valve 2' is open until the pressure from the green fluid increases and reaches the threshold pressure. Upon reaching the threshold pressure, the membrane of 'valve 2' deforms toward the red fluid channel, blocking the red fluid flow. In this instance, the green fluid starts to flow toward the outlet through 'valve 1'. Likewise, the outlet flow switches autonomously due to alternative opening and closing actions of the fluidic transistors. The switching frequency depends on the inlet pressure and the geometrical parameters of the microchannels, microchambers, and membranes. The main drawback is the lower controllability of the duty cycle, which is the time that each fluid is drawn to the outlet channel.

Kim et al. developed a fluidic oscillator consisting of 3-terminal switch valves.[224] Its function in various duty cycles was suitable for cell signaling studies. Unlike in 4-terminal valves, the working fluid of one valve does not pass through the other valve to generate fluid oscillations. Kim et al.[40] developed a self-switching pulsatile flow circuit using an array of fluidic transistors, (Figure 7C). When the source pressure of 'valve 2' is greater than the gate pressure, the red fluid flows through the drain to the outlet while maintaining the gate pressure of 'valve 1'. However,

the pressure at the inlet of 'valve 1' increases due to the constant flow from the syringe pump. When the inlet pressure exceeds the gate pressure, 'valve 1' switches on, and the green fluid flows toward and exits the outlet while maintaining the gate pressure of 'valve 2'. Hence, a pulsatile flow is autonomously generated by providing a continuous flow at the inlets. The constant water-head pressure, exerted by a column of liquid due to gravity, provided the continuous flow.[40] The same gravity-driven source was used for the sub-circuits, but the oscillation frequencies were independent. In addition, the fluidic resistance constrained the flow switching period (0.1 s – 5.9 h) and the flow rate (2 μL min^{-1} – 2 mL min^{-1}) of a similar fluidic oscillator.[215] Furthermore, the same group developed a stepwise waveform generator by serially connecting a fluidic oscillator and a diode pump.[225] The diode pump consisted of two fluidic transistors and two check valves as diodes to maintain a unidirectional flow. The gravity-driven constant pressure was converted to pulsatile pressures in the stepwise waveform generator using the oscillator. The diode pump utilized the pulsatile pressure to generate stepwise pressures. This device could obtain the step size from 215 to 431 Pa and the duration of the pressure step from 26 to 181 s independently.

Besides the microvalves and transistors actuated by hydraulic forces, active microvalves actuated by pneumatic pressure and magnetic forces can also generate periodic flows in the microenvironment.[226,227] Aeroelasticity is the deflection of the flexible membrane due to airflow.[216] When the pressure of the external airflow exceeds the pressure inside the microchannel, the flexible membrane deflects upwards (Figure 7D). This process generates a spontaneous pressure drop in the microchannel and demonstrates the 'ON' status of a transistor. Then, the air pressure in the pneumatic actuation channel will drop because air is released from the gap between the membrane and the nozzle. As a result, the fluidic pressure inside the microchannel pushes the diaphragm toward the nozzle and closes the air-releasing gap, corresponding to the "OFF" condition of the fluidic transistor. Similarly, electromagnetic force deflects flexible membranes responsive to magnetic field variations, which can be generated by an electromagnet. Following on this mechanism, Zhao et al.[228] developed an on-chip multi-pattern periodic flow generator by introducing an alternating pressure into a constant pressure using electromagnetic actuation. Their periodic flow generator has demonstrated high controllability and has a small footprint.

Intrinsically active hydrogels have been used for chemo-fluidic transistors that respond to input chemical signals such as concentrations of organic solvents, ions, pH value, and the presence of biomolecules.[229,230] This phase transition of hydrogels in relation to varying alcohol concentrations was employed to develop a microfluidic oscillator.[231] The bidirectional coupling of fluid flow and chemical process added additional controllability. A chemo-fluidic transistor with an elastic membrane actuated using hydrogel was developed (Figure 7E).[42] When the activated hydrogel component expands, it restricts the fluid flow by deflecting the membrane toward the microchannel. Conversely, when the hydrogel contracts, the membrane retracts, and the microchannel cross section expands so that the reduced fluidic resistance can enable the fluid to flow freely inside.

3.3. Fluidic Capacitance

A capacitive element can store potential energy by altering its shape or size. The capacitive element can deform under applied pressure, storing a specific amount of fluid and converting the kinetic energy of the fluid into capacitive potential energy (**Figure 8A**). The stored potential energy can be released to expel the stored fluid.[81,232] Repetition of such cycles results in periodic flows. In a microfluidic system, the fluidic capacitance can be external or internal. External capacitance comes from the flexibility of tubes or components related to external peripherals not integrated into the microfluidic chip.[91,233] Internal capacitive elements include elastomeric membranes and trapped air bubbles in microchannels.[222,234,235]

Hydroelasticity, the interaction between flexible structure and fluid flow, is commonly used to produce fluidic capacitance-based periodic flows.[236] A flexible structure introduces nonlinearity to the fluid flow, and the pulsating frequency depends on the elasticity and the geometrical parameters of the membrane. Wu et al.[43] developed a simple oscillatory flow generator consisting of a microchamber, membrane, and microchannel but no outlet (Figure 8B). A constant pressure source was connected to the inlet through a solenoid valve. When the valve is switched on, the fluid flows from the inlet toward the membrane. The membrane deflects, and the elastic force is increased. When the valve is switched off, the elastic force pushes the flow backwards, generating an oscillatory flow in the microchamber. In another study, an elastic diaphragm was placed inside a stepped circular cavity with circumferentially distributed three grooves (Figure 8C).[44] The device was fabricated using a PMMA-based layer-by-layer method, and the diaphragm was made of silicone rubber. This diaphragm separates the microchamber in the second PMMA layer (from the bottom) into two: the main chamber on the inlet side of the membrane and the secondary chamber on the outlet side. Initially, the elastic diaphragm is flat. When the fluid is supplied to the inlet with a constant pressure, it flows to the main chamber and deflects the diaphragm toward the secondary chamber. The fluid flows over the edge of the diaphragm. Then, fluid drains into the secondary chamber and the grooves ensure an uninterrupted fluid flow. The deflection of the diaphragm changes the hydrodynamic drag and lift forces. In addition, the elastic forces tend to restore the diaphragm to its original shape. All these forces are at an equilibrium at low pressures, resulting in a steady flow. When the supply pressure increases, the membrane deflects further downstream. Once the inlet pressure exceeds a threshold, the inertial force deflects the elastic membrane further over the equilibrium point, causing it to overshoot the balancing point. Then, the lift and elastic forces push it back. The incoming flow deflects the diaphragm again toward the secondary channel, leading to another inertial overshoot. This cycle repeats, producing periodic movement of the diaphragm, along with the storage and release of elastic energy. Hence, a pulsatile flow is generated at the outlet.

Meanwhile, the compressibility of air bubbles was used to produce periodic flows in microfluidic devices.[237] Figure 8D shows an air bubble-based oscillatory platform developed using a periodic pneumatic pressure source at the inlet and a sealed glass capillary fixed at the outlet of the microfluidic device.[45] When the pressure source pushes the fluid through the pipette tip into

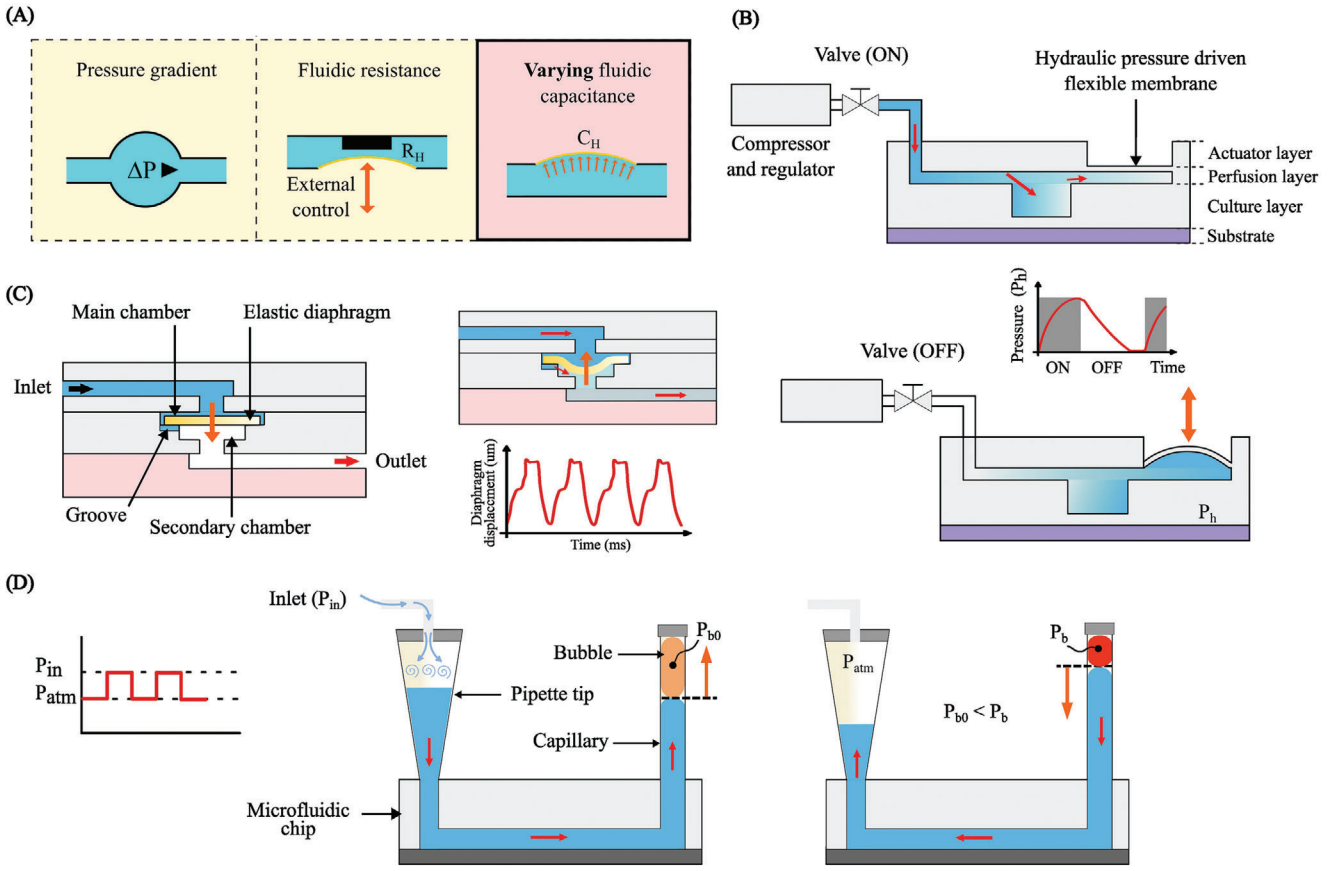

Figure 8. A) Fluidic capacitance-based periodic flow generation. B) Elastic energy stored by the membrane at the pumping stage generates reverse flow when the pressure supply is switched "OFF". Reproduced with permission.[43] Copyright 2019, John Wiley and Sons. C) Oscillatory deflection of an elastic diaphragm by a constant pressure produced periodic flows through grooves. Reproduced with permission.[44] Copyright 2012, The Royal Society of Chemistry. D) A trapped air bubble compresses when pressure is supplied and expands upon removing the pressure, generating a backward flow. Reproduced with permission.[45] Copyright 2018, The American Institute of Physics.

the device, the air bubble trapped in the capillary is rapidly compressed. When the pressure at the inlet balances that in the air bubble, the liquid is at an equilibrium. If the pressure supply at the inlet is switched off, the compressed air bubble pushes the liquid backwards. Hence, the air bubble acts similarly to the charging and discharging process of a capacitor in electronic circuits and produces a periodic flow.

4. Applications

Periodic flows in microfluidics have a wide range of applications that enhance the functionality and efficiency of microfluidic systems. For example, these flows improve fluid mixing by creating oscillatory patterns, promoting thorough mixing.[238–241] Besides, periodic flows offer precise control over droplet size and formation, independent of Rayleigh–Plateau instabilities for droplet generation.[46,242] They can also enhance heat transfer for cooling microelectronic devices.[243–245] Moreover, periodic flows replicate natural pulsatile conditions, improving cell culture and biological studies.[246–248] This section elaborates on the applications of periodic flow in microfluidics, including fluid mixing, heat transfer, droplet/bubble generation, particle manipulation, filtration enhancement, biomimicry, fluid rheology measurement, and microstructure fabrication.

4.1. Fluid mixing

In microfluidics, the Reynolds number (*Re*) is typically very low, resulting in laminar flow and challenging mass transfer and mixing.[249] Periodic excitations applied to the fluid flow can significantly enhance mixing with minimal impact on device geometry and setup, allowing for adjustable mixing conditions.[46,112,250,251] Mixing methods can be active, using external energy, or passive, employing baffles, mixing structures, or curved geometries.[29] An oscillatory baffled reactor (OBR) combined active mixing through periodic flow with passive mixing via baffles.[126] Increasing the oscillation frequency boosted mixing intensity and vortex propagation. For example, in desulphurizing dibenzothiophene (DBT) in diesel, sulfur removal improved from 9% to 35% as the oscillation frequency increased from 0 to 4 Hz. Similarly, in desulphurizing sour, heavy naphtha, increasing the oscillatory Reynolds number (Re_o) from 175 to 315 raised the conversion rate from 79.3% to 93.7%.[252]

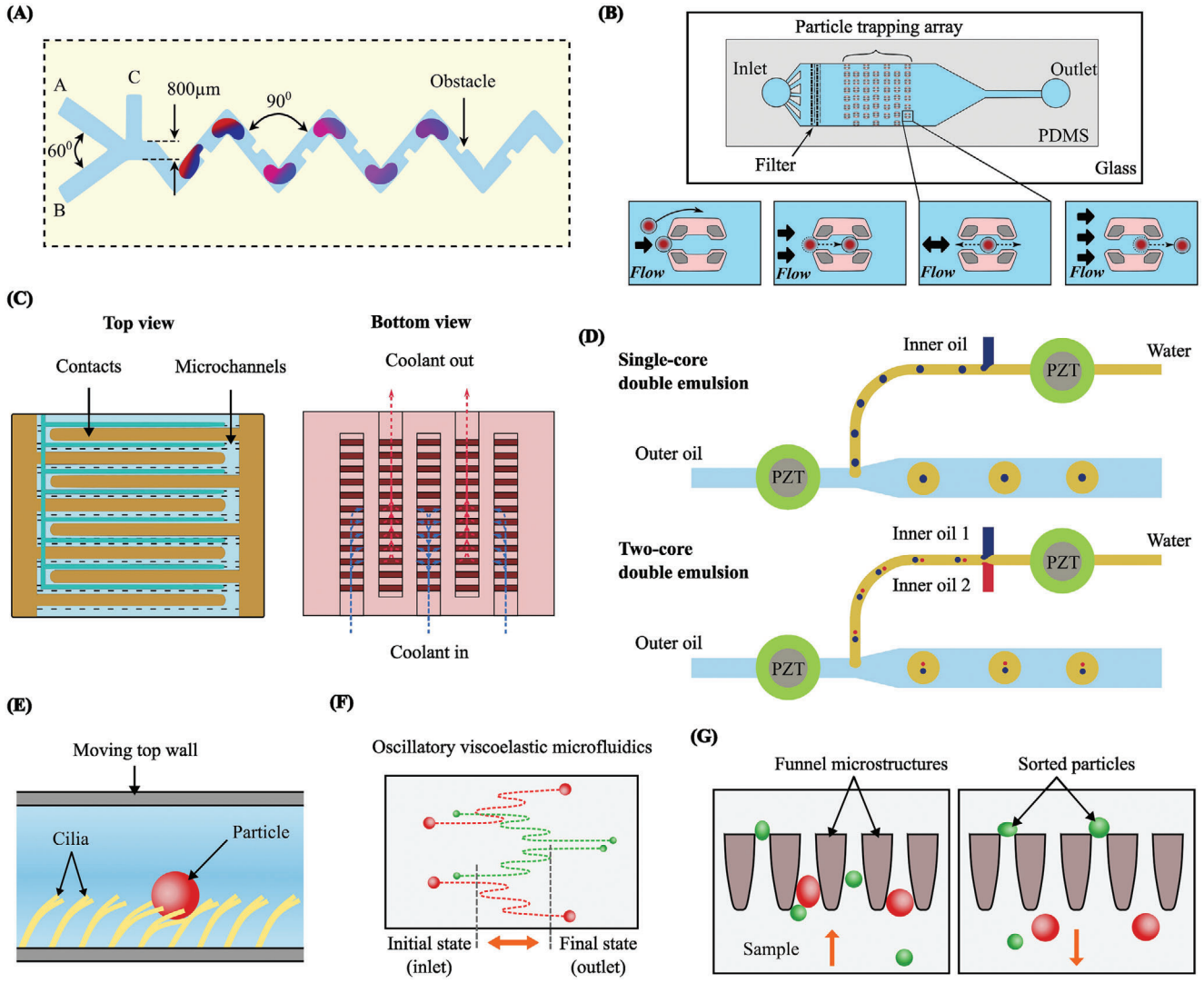

Figure 9. Applications of periodic flows in microfluidics. A) Micro-mixing in a V-shaped microchannel using pulsed discontinuous flow. Reproduced with permission.[254] Copyright 2024, Elsevier. B) Oscillatory flow-based immunostaining in an immunoassay to detect ZIKV. Reproduced with permission.[32] Copyright 2019, Elsevier. C) Cooling electronic devices using elastic turbulence of viscoelastic fluid in serpentine channels. Reproduced with permission.[255] Copyright 2020, Springer Nature. D) Synchronized generation of single-core and two-core double emulsions. Reproduced with permission.[256] Copyright 2019, Elsevier. E) Transporting sticky particles by coupling oscillatory flow with artificial cilia. Reproduced with permission.[257] Copyright 2014, The Royal Society of Chemistry. F) Oscillatory viscoelastic focusing and separation of micro and submicro species. Reproduced with permission.[25] Copyright 2020, The American Chemical Society. G) Oscillatory flow reduces clogging in microfiltration. Reproduced with permission.[258] Copyright 2012, The Royal Society of Chemistry.

Introducing induced vibration to an elastic structure improves controllability and enhances mixing. Loe and colleagues[250,253] used a feedback-type fluidic oscillator and vortex shedding with a cylindrical structure to numerically study optimal flow regulation. The team applied phase reduction theory to evaluate device geometric parameters via the phase-sensitivity function, concluding that this method optimizes the perturbation signal and enhances mixing. Curved channels form Dean vortices that enhance radial mixing. Combining periodic flow with a curved microchannel reduced the axial dispersion number tenfold, improving transverse mixing.[29] Wang et al.[254] achieved a high mixing index (≈95% at the outlet) by introducing discontinuous flow to a V-shaped microchannel in a microfluidic device, with square-shaped obstacles inside the microchannel (**Figure 9**A), improving the mixing efficiency from 89% to 95%. Smaller volumes of discontinuous flow and higher inlet velocities improved mixing. Smaller volumes need less collision, rotation, and diffusion to complete mixing. However, a very low volume created a droplet at the corner of the microchannel and may stop its movement along the microchannel. Furthermore, curves and obstacles in the channel caused stronger self-diffusion effects at higher velocities, reducing mixing time.

Periodic oscillations effectively mix and bind streptavidin-conjugated particles with fluorescence-labelled biotin samples in an immunoassay for detecting the Zika virus (ZIKV), which

requires only 10 µl of the sample and takes just 10 min to complete (Figure 9B).[32] Quantitative analysis shows that oscillatory flow-based immunostaining is more efficient than conventional static and continuous flow staining.[45] In the study, static staining took 15 min with 2 µl of reagent, while continuous flow staining required 12 min and 4 µl. In contrast, oscillatory-based immunostaining needed only ≈5 min and 2 µl of reagent to achieve the same results. Besides, oscillatory flow coupled with swirling enhances the mixing of solvent and antisolvent, which initiates recrystallisation in core-shell droplet formation.[259] Oscillatory flows can reduce channel blockage, provide safe mixing, and improve the efficiency of molecular diffusion by shortening the delay time.

4.2. Heat Transfer

Excessive heat in microelectronics, photovoltaic cells, infrared detectors, and laser diodes requires temperature regulation (Figure 9C).[255] Heat pipe technology is widely used in microscale cooling devices.[260,261] This technology utilizes cooling agents in interconnected serpentine microchannel networks to transfer heat. The thermophysical properties of the working fluid directly influence its motion. Heat transfer at the microscale can be enhanced using elastic turbulence by adding small concentrations of high-molecular-weight polymer to a Newtonian solvent.[262,263] This addition induces non-linear effects and elastic instabilities at low Reynolds numbers in serpentine microchannels, significantly enhancing convective heat transfer by up to 300%.[264] The use of shear-thinning and constant-viscosity Boger solutions further improves convective heat transfer in serpentine microchannels, with enhancements reaching 380% compared to similar Newtonian fluids.[249] Recently, flexible polymer-based micro heat pipe devices have emerged. In oscillating or pulsating heat pipe networks, temperature differences and phase changes facilitate heat transfer from the evaporator to the condenser elements without external driving forces.[265]

4.3. Droplet/Bubble Generation

Droplet formation involves two immiscible liquids: the dispersed phase, which forms the droplets, is injected into the continuous phase, which flows around and encapsulates the droplets.[266] These droplets play a significant role in cell encapsulation and manipulation,[267,268] single-cell analysis,[269,270] particle synthesis,[271] emulsification,[272] etc. Various passive and active techniques are used to generate droplets in microfluidics.[273] Passive techniques for droplet generation rely on the natural development of Rayleigh–Plateau instabilities to initiate droplet formation.[274] The pulsatile condition offers additional control over droplet formation by eliminating reliance on the growth of Rayleigh–Plateau instabilities.[46] Pulsating the continuous-phase flow in a T-junction droplet generator could govern the droplet formation process.[275] The single perturbation source (elastic diaphragm) decouples droplet size, generation frequency, and fluid properties. At nearly fixed operating pressure and frequency, the droplet volume increased linearly with flow rate over a broad viscosity range (1 – 60 cP), allowing easy tuning. This method enabled the synchronous production of droplets with largely different volumes and viscosity, facilitating precise one-to-one droplet coalescence.

Using pulsatile airflow to actively control droplet ejection significantly enhances the tunability of droplet parameters.[276] Pulsatile perturbation enhanced the control of droplet size, ejection frequency, and velocity. In the synchronous regime, the droplet generation frequency corresponded entirely to the external pulsation frequency. This method produced highly monodispersed droplets and was effective for fluids with viscosities up to 100 cP. The method also expanded the regulation range of droplet sizes from 10 to 60 nL, enabling precise and high-frequency droplet ejection. Besides, the droplet generation frequency can be directly synchronized with the frequency of a piezoelectric actuator, while droplet spacing is controlled by the continuous-phase flow rate (Figure 9D).[256] Within the resonance range, the device performed on-demand droplet generation at high frequencies up to 3.3 kHz. Double-emulsion droplets were produced with tunable volumes for the core droplet and middle-phase fluid.

Compared to the droplet generation in oil-in-water or water-in-oil systems, aqueous two-phase systems (ATPSs) exhibit over 500 times lower interfacial tension, making it more challenging.[277] Ziemecka et al.[278] integrated a piezo-electric bending disc into the microfluidic device and studied the influence of amplitude and frequency on water-in-water droplet generation. Mechanical perturbations were introduced to the dispersed phase, allowing flow rate-independent droplet size modulation. Different droplet behaviors were observed by varying the frequency from 2 to 50 Hz and the amplitude from 3 to 25 V. Higher frequencies above 20 Hz resulted in the formation of monodispersed droplets, while lower frequencies produced polydispersed droplets. The most effective regime was between 20 to 50 Hz, where reproducible monodisperse droplets with diameters below 60 µm were consistently formed. The variation in amplitude had a very slight effect compared to the significant impact of frequency changes. Similarly, Sauret et al.[279] used a mechanical vibrator to pulse the flexible tube that transported the dispersed phase and formed water-in-water droplets. This ATPS generated droplets and double emulsions in the glass microcapillary devices. Monodisperse droplets were induced for voltage above 3 V and at the frequency range from 5 to 9 Hz. In the case of double emulsion generation, a modified glass microcapillary device was used to introduce the inner, middle, and outer fluids. The size of droplets and the number of inner droplets were precisely tunable by regulating the vibration frequency, amplitude, and flow rates. Furthermore, oscillatory flows are used to actively regulate gas-liquid Taylor flow (or Taylor bubbles) in microfluidics. Zhang et al.[280] applied a solenoid valve with a 0.05 s response time to provide pulsations to the gas feed in rectangular waves with 0 – 20 Hz frequencies. Bubble formation (bubble length and velocity) at the T-junction showed reliance on surface tension, shear stress, and dynamic pressure, which were significantly affected by gas feed pulsations. Furthermore, Wang et al.[281] proposed a rotating switch valve-based perturbation to the gas feed to generate pulsations at kilohertz frequencies. Both the Taylor bubble formation and liquid-in-gas droplet generation are governed by the pulsations to the gas feed.

4.4. Particle Manipulation

Precise manipulation, such as focusing, separation, and fractionation of bio-particles, is an indispensable capability of microfluidics, with applications in clinical diagnosis, cell sorting and analysis, drug discovery, etc.[282–285] Particle manipulation techniques can benefit from periodic flows in microfluidics.[45,286,287] Tripathi et al.[257] studied the coupling of oscillatory flow with artificial cilia to transport sticky particles in microchannels (Figure 9E). This method expelled particles from the ciliated surface up to a critical adhesion strength, resulting in faster movement than non-oscillatory flow. The non-actuated artificial cilia follow the motion of the fluid at ≈12 Hz frequency, reducing the requirement for bulky and sophisticated equipment. The smaller particles such as fungi, bacteria, viruses, and other pathogens or blood components such as platelets and exosomes require drastically longer microchannels for inertial focusing.[116] Oscillatory flows were applied in inertial microfluidics to enable virtually "infinite" channel length to focus 500-nm particles and a submicron bacterium (≈0.8 μm).[26] Asghari et al.[25] developed sheathless oscillatory viscoelastic microfluidics as an effective method for focusing and separating micrometer and sub-micrometer species, demonstrated by isolating p-bodies from biofluids, focusing λ-DNA, and focusing extracellular vesicles (Figure 9F). In this study, the larger particles (10 μm) focused near channel walls, while the smaller particles (5 μm) particles focused near the centerline, and the smallest particles (1 μm) aligned at the centerline at an oscillation frequency of 2 Hz. Besides, oscillatory flows were integrated with insulator-based dielectrophoresis[57] and negative magnetophoresis[161] to focus particles and cells.

4.5. Filtration Enhancement

Microfiltration uses porous membranes or microstructures to separate particles and cells.[288–292] In 1993, Howell et al.[293] reported the significance of using oscillatory flows in harvesting Yeast cells. They investigated three filtration systems to filter Yeast cells using oscillatory flows with frequencies ranging from 0 to 25 Hz. In another study,[294] the effects of oscillating the porous membrane and working fluid were investigated at a range between 10 to 50 Hz. Oscillations significantly improved the flux over conventional filtration between 125% to 320%, leading to reduced membrane fouling and concentration polarization. Wang et al. utilized an oscillator to generate pulsatile flow with varying frequencies and pressures, inducing high shear rates, surface souring, and back-flushing effects.[295] This setup effectively eliminates concentration polarization and micropore clogging while hindering the formation of the fouling layer, resulting in minimized membrane fouling and a 30% reduction in microfiltration process time. Despite the dynamic filtration, constant supply pressure avoids the complex rotational or vibrational mechanisms. Compared to static filtration, permeate flux significantly improved. Pulsatile filtration was used to filter extracellular vesicles directly from human whole blood samples for early cancer diagnosis.[296] Two porous membranes with porous sizes of 600 nm and 20 nm filtered cells and extracellular vesicles, respectively. Aeroelastic deformation of a flexible membrane generated the forward and reverse flow, while the check valve ensured a net forward flow. The reverse flow levitated the bioparticles away from the membrane, reducing filter fouling and particle aggregations.

Carefully designed microstructures, such as funnels and traps, allow particles smaller than a specific threshold to pass while retaining larger particles. McFaul et al.[258] developed a device consisting of several layers of linear funnel arrays, as depicted in Figure 9G, to separate cells in whole blood based on size and deformability. These experiments utilized oscillatory flow to minimize clogging – the undesired deposition of particles on microchannel walls. Periodic flows cause particles to change direction over time, reducing the likelihood of clogging compared to continuous-flow devices. Dincau et al.[53] found that pulsatile flows ranging from 0.001 Hz to 0.1 Hz significantly reduced clogging, with complete mitigation at 0.1 Hz, demonstrating the effectiveness of periodic flows in minimizing clogging. Additionally, liquid-liquid extraction, a separation technique used in various industries, benefits from oscillatory flows.[237] Lestari et al. utilized switchable hydrophobicity to separate dimethyl cyclohexylamine in a hexadecane-toluene mixture.[297] The team found that higher oscillatory flow velocities improved the extraction rate and reduced extraction time.

4.6. Biomimicry

In microfluidics, biomimicry involves imitating biological functions to replicate dynamic flows in systems such as the blood circulatory system, digestive tract, and urethral transport.[159] Organ-on-a-chip (OoC) devices that replicate human organ functions offer insights into physiological behaviors, treatment procedures, disease diagnosis, and drug discovery.[298] Producing the hemodynamic waveform shown in **Figure 10A**, is often studied due to its broad applications.[50,299]

Microfluidic devices were designed to mimic tissue development in microenvironments.[304] For example, growing human umbilical vein endothelial cells and embryonic stem cells requires heartbeat-like pulsations in fluid flow, which was generated using a cardiac pump, to study cell responses to fluid dynamics.[305] Ex vivo heart perfusion (EVHP) devices, essential for heart transplants, need precise pulsatile flow regulation to maintain donor heart viability (Figure 10B).[300] The aorta's role in flow regulation is mirrored in EVHP settings using elastomeric tubes.[299] These devices should ideally self-regulate pulsatile flows, similar to physiological conditions. Jen et al.[306,307] demonstrated passive self-regulation using knitted reinforced materials around elastomeric tubes. Heartbeat-like pressure stimuli are also crucial for developing liver organoids for diagnostics, drug discovery, and regenerative medicine.[43]

Naturally, the fluid flow in the lymphatic system is pulsatile.[308,309] Selahi et al.[310] developed a lymphangion-chip to support co-culture and bidirectional signaling of lymphatic endothelial cells (LECs) and muscle cells (LMCs). This was achieved by wrapping multiple uniform LMC layers around a single LEC layer, forming a lumen (space inside a tubular membrane structure). Then, a pulsatile fluid flow was provided to imitate the physiological lymphatic vascular functions mediated by intracellular calcium $[Ca^{2+}]_i$ (Figure 10C).[301] The lymphangion-chip demonstrated the significance of cyclic

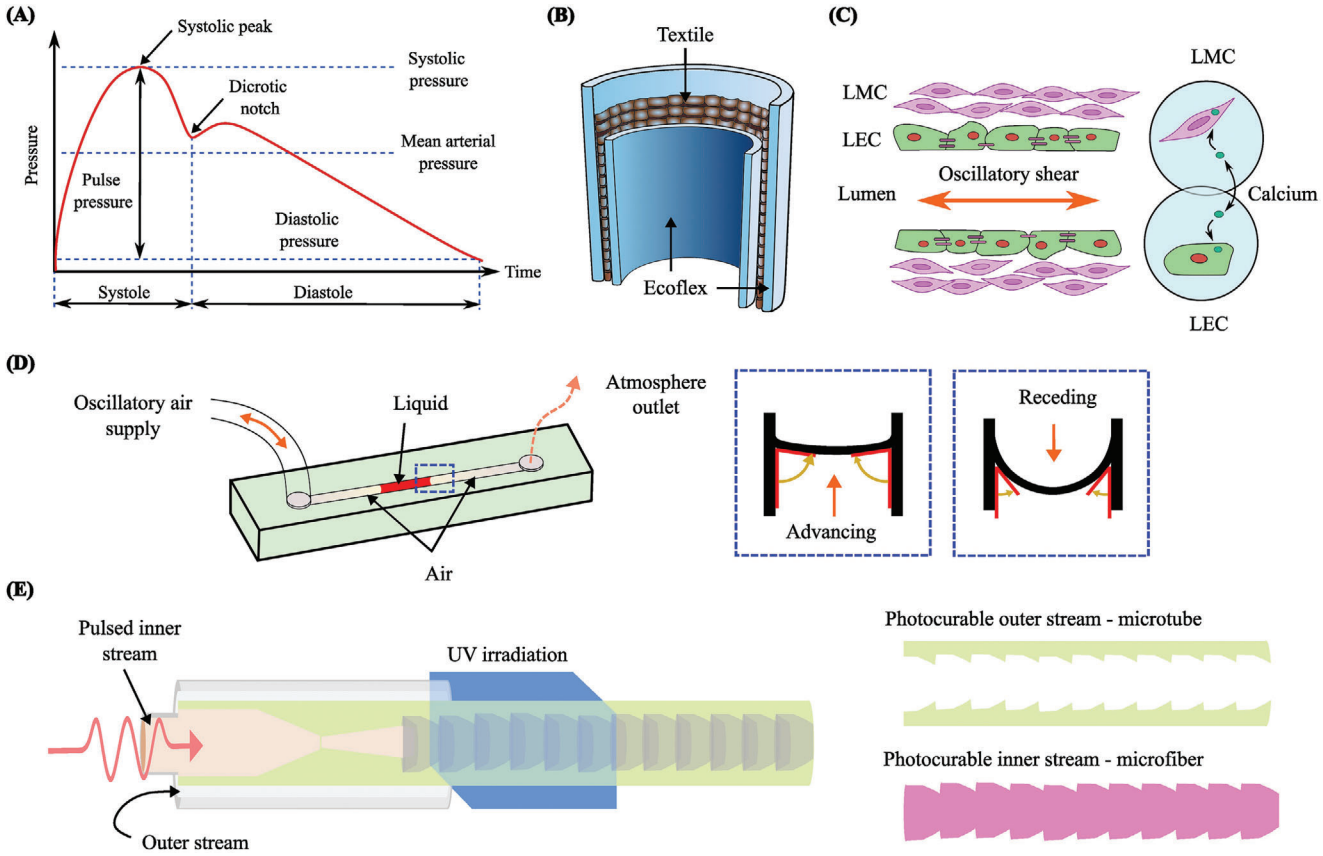

Figure 10. Further applications of periodic flows in microfluidics. A) Symbolic arterial blood pressure waveform. Reproduced with permission.[299] Copyright 2020, The Public Library of Science. B) Mimicking the human aorta using fabric-reinforced elastomer tubes. Reproduced with permission.[300] Copyright 2019, The American Chemical Society. C) Intracellular calcium dynamics of lymphatic endothelial and muscle cells in a lymphangion-chip under pulsatile flow. Reproduced with permission.[301] Copyright 2022, The Royal Society of Chemistry. D) Measuring rheological properties of viscoelastic fluids using oscillatory movements of the air-liquid surface. Reproduced with permission.[113] Copyright 2021, Frontiers. E) Producing microtubes with microstructures in the inner wall and fabricating microfibers with repeating structural components. Reproduced with permission.[302] Copyright 2024, The National Academy of Sciences. Reproduced with permission.[303] Copyright 2024, Springer Nature.

mechanical forces in regulating intracellular calcium. This can be used as an analytical biomarker of mechanotransduction within LECs and LMCs that are useful for pathology. In addition, Wang et al.[138] used periodic flows to enhance intercellular calcium transfer in osteogenesis, finding that low-frequency oscillatory flow significantly improves calcium responses in bone cells compared to unidirectional flows, thus promoting bone tissue formation.

4.7. Fluid Rheology Measurement

Flow behavior and deformation characteristics of fluids under applied external forces refer to "rheology".[311] Measuring rheological properties such as yield stress,[312] relaxation time,[313] elasticity,[314] dynamic permeability,[315] and viscoelasticity,[316] is essential in assessing complex fluids,[317,318] designing machines and devices,[319] and process optimization,.[320] Conventionally, properties under shear and extensional stresses are measured using shear and extensional rheometers, respectively. These bulky rheology instruments suffer from limited frequency range and probed moduli, heterogeneity, and cost.[321] Moreover, they are not suitable for biological samples because of the need for a large amount of samples and the edge effects.[322] Furthermore, these instruments are limited in assessing the "longest relaxation time", which is a critical parameter in coating, drag reduction, droplet formation, and mixing applications.[323] Microfluidic rheometry has emerged to mitigate the limitations of conventional techniques.[324,325]

Oscillatory flow rheometry is particularly interesting due to the small sample volume required.[326] The intra-cycle microstructural changes in colloidal gels were studied using an oscillatory flow-based rheometry.[327] Oscillatory shearing in complex fluids was studied using Brownian dynamics simulations and the sequence of physical processes (SPP) technique to quantify the correlations. The rigidity concept linked microstructural changes to rheological behavior. In the study, the colloidal gels exhibited complex nonlinear stress responses under large-amplitude oscillatory shearing. Vazques-Vergara et al.[113] investigated the rheological properties of viscoelastic fluids using oscillatory flow rheometry (Figure 10D). A piezoelectrically actuated elastic membrane pumped air to the inlet, and a short liquid

length was placed in the microchannel as the working fluid. Resonance in dynamic permeability at the air-liquid interface was studied for three polyethylene oxide polymer solutions as model viscoelastic fluids. The oscillatory flow operated between 0.5 Hz to 200 Hz frequencies at pressure drop amplitudes from 225 to 900 Pa. Elastic turbulence, a chaotic fluid motion observed in non-Newtonian fluids such as blood,[328,329] can result in complex fluid dynamics.[330] The influence of elastic turbulence on the rheological measurement of the pulsatile blood flow is vital for understanding complicated hydrodynamics and fluid-structure interactions in an aneurysm.[331]

4.8. Microstructure Fabrication

Innovative microfabrication techniques have significantly driven recent advancements in microfluidics. The time-dependent nature of periodic flows features unique advantages in microfabrication and producing materials with microstructures. Localized electrochemical deposition micro additive manufacturing (LECD-μAM) combines localized electrochemical deposition and closed-loop control of atomic force servo technology.[332] Applying a pulsatile pressure to drive the electrolyte solution in LECD-μAM allowed layer-by-layer deposition and enhanced the spreading and sedimentation rates.[333] This method was successful in fabricating microstructures such as lattice monomers, pillar arrays, thin walls, high-aspect-ratio (≈500) wires, helical springs, and hollow tubes.[334]

Injecting fluid into a second co-flowing immiscible fluid creates a jet that either remains stable or breaks into droplets. A corrugated jet was observed in a two-phase flow at significantly low interfacial tension.[277] A pulsation of the inner stream formed complicated patterns and corrugations. Yang et al.[302] manufactured hollow microtubes using a co-flow microfluidic spinning system coupled with a programmable piezoelectric vibrator (Figure 10E). This system consisted of inner and outer streams, where the photocurable outer layer was exposed to a UV light beam, forming the microtube structure. These microtubes featured round outer walls and unique anisotropic inner walls with periodic micro-corrugations. The overlapped truncated cone-shaped cavities along the axial direction were formed due to the pulsed inner stream, and the pitch and thickness of the cavities were adjustable by the electrical frequency and voltage. The inner diameter of the tube was regulated by the flow rates of the inner and outer phases. These flexible microtubes were applied for precise directional fluid transport.

Microfluidics can produce microfibers with specific shapes, structures, and functionalities due to its precise control over fluid flows. Yang's group developed flexible hemline-shaped microfibers by infusing the photocurable solution as the inner stream and water as the outer layer under a pulsatile flow.[303] The fabricated hemline-shaped microfibers featured axially aligned cavities with sharp edges and annularly connected wedge corners due to piezoelectric pulsations to the inner stream. Unidirectional fluid transport was observed on the hydrophilic substrate of a single microfiber. More interestingly, a pair of microfibers with the same or opposite corner orientations demonstrated unidirectional fluid transport independent of the type of liquid or surface wettability. A similar piezoelectric microfluidic platform enabled consecutive spinning of functional microfibers with programmable spindle-knots.[335] These knot microfibers remain stable even when tied, bent, or coiled. Their axial non-uniformity enabled long-distance transport of water and unidirectional/bidirectional droplet transport. Adjusting the piezoelectric and microfluidic parameters allowed the generation of knot fibers with customizable configurations, including uniform, gradient, and symmetrical knots, on demand.

5. Discussion and Perspectives

The present paper explores the behavior, generation techniques, and applications of periodic flows in microfluidics. First, we explained the fundamental theory of periodic flows. Then, we discussed the hydraulic-electric analogy and its usefulness. We classified the techniques for generating periodic flows based on pressure gradient, fluidic resistance, transistor, and capacitance, and elaborated their working mechanisms. Finally, we reviewed the applications of periodic flows, such as fluid mixing, droplet/bubble generation, biomimicry etc. Although considerable progress has been achieved, the field is still at its early stage. Future research efforts are needed to exploit the full potential of periodic flows in microfluidics by addressing current challenges in mechanisms, fabrication, miniaturization, and integration.

Generating periodic flows across a wide frequency range is a major challenge in microfluidic systems. The ideal method should precisely control flow rate and direction across various frequencies. Syringe pumps, pneumatic pressure controllers, electromechanical relay valves, and fluidic oscillators are typically used for frequencies below 10 Hz.[31,39,113] Syringe pumps are the most accessible devices, but they commonly have large response times, limiting their ability to generate high-frequency dynamic flow profiles. Conventional peristaltic pumps are easy to operate, but produce undesired pulses that challenge the precise modulation of flows. For frequencies between 10 Hz and 1000 Hz, high-speed valves, piezoelectric elements, mechanical motors, air bubble displacement, loudspeaker diaphragms, or automated droplet trains are used.[31,113] Although devices that use piezoelectric elements are widely studied, this method still has much space for further refinement in terms of precision, efficiency, and adaptability.

Integrating periodic flow generation with microfluidic systems presents opportunities and challenges. Seamlessly incorporating flow generation mechanisms within microfluidic devices can enhance their portability and functionality. One promising direction is the development of fully integrated, self-contained microfluidic chips that include on-chip flow generation, sensors, and a control system. This integration would simplify system design, reduce external dependencies (e.g., power supplies, signal generators, amplifiers), and improve overall system efficiency. Miniaturizing macroscale periodic flow generators is challenging due to their complex features, and new generation mechanisms based on the fluid-structure interaction should be developed at the microscale, such as hydroelasticity and aeroelasticity.[44,216]

Exploring new materials and microfabrication techniques could lead to robust and miniaturized flow generation devices. Smart materials, such as shape-memory alloys and responsive polymers, have been employed to create adaptive systems that adjust flow patterns in response to environmental changes or

stimuli.[41,42] This adaptability enhances reliability and versatility in diverse microfluidic applications. In addition, light-sensitive materials are significant due to the ability to remote actuation, yet the present studies are limited to very low frequencies (i.e., large response times). More effort should be put toward enhancing their response speed and sensitivity. Besides, future research endeavors should explore mechanisms of generating periodic flow based on novel materials, such as liquid metals,[336] MXenes,[337] and metal-organic frameworks (MOF).[338] Regarding fabrication techniques, the advancement of 3D printing-based additive manufacturing techniques, especially two-photon polymerization, brings unprecedented microfabrication capability and resolution for complex 3D architectures at the micro and nanometer scale.[339–342] This fabrication capability removes the limitations of 2D layer-by-layer design and fabrication of traditional photolithography and soft lithography techniques, enabling the one-step fabrication of complex 3D structures. This promises to achieve higher device reliability and performance.

Micro elastofluidics, an emerging field studying fluid-structure interactions at molecular and microscopic scales, shows promise for liquid handling and biological interfacing.[343–346] Advances in flexible materials enable innovative fluidic capacitance-based devices and microfluidic transistors to generate periodic flows. Future research should prioritize developing novel polymers, elastomers, and hybrid materials that can withstand repeated deformation while maintaining their structural integrity and functional properties. Besides, the integration of flexible microfluidics with electronic components, such as sensors and actuators, could enable real-time monitoring and control of periodic flows. This could lead to the development of smart microfluidic devices that automatically adjust flow parameters in response to changes in the system or external conditions. Such integration would be particularly beneficial for applications requiring precise flow regulation, such as tissue engineering and organ-on-a-chip platforms.

In summary, periodic flows in microfluidics hold immense innovation potential across various fields. Understanding the fundamental mechanisms of periodic flow generation and expanding their applications is crucial. By developing advanced generation methods, new materials and fabrication methods and seamlessly integrating them within microfluidic systems, researchers can unlock new capabilities, functionalities and applications. Continued interdisciplinary collaboration and the incorporation of emerging materials will be key to advancing this promising research area.

Acknowledgements

The authors acknowledge the support from the Australian Research Council (ARC) Australian Laureate Fellowship (Grant No. FL230100023) and ARC DECRA fellowship (Grant No. DE210100692).

Open access publishing facilitated by Griffith University, as part of the Wiley - Griffith University agreement via the Council of Australian University Librarians.

Conflict of Interest

The authors declare no conflict of interest.

Author Contributions

J.Z. and N.-T.N. performed conceptualization, supervision, and project administration. A.M. performed formal analysis, wrote the original draft, and visualization. U.R., S.H., H.C., H.M., and X.K. performed visualization. J.Z., N.-T.N., Q.T.T., and H.M.X. performed reviewed and edited the draft. J.Z. and N.-T.N. performed funding acquisition. All the authors provided critical feedback and read and approved the manuscript.

Keywords

hydraulic-electric analogy, oscillatory flows, periodic flow generation, pulsatile flows

Received: June 8, 2024
Revised: August 24, 2024
Published online: September 9, 2024

[1] G. M. Whitesides, *Nature* **2006**, *442*, 368.
[2] D. K. Abeywardana, A. P. Hu, Z. Salcic, *Sens. Actuators, A* **2017**, *263*, 8.
[3] Y. Song, B. Lin, T. Tian, X. Xu, W. Wang, Q. Ruan, J. Guo, Z. Zhu, C. Yang, *Anal. Chem.* **2018**, *91*, 388.
[4] E. K. Sackmann, A. L. Fulton, D. J. Beebe, *Nature* **2014**, *507*, 181.
[5] N. Frey, U. M. Sönmez, J. Minden, P. LeDuc, *Nat. Commun.* **2022**, *13*, 3195.
[6] N. Convery, N. Gadegaard, *Micro Nano Eng.* **2019**, *2*, 76.
[7] J. Zhang, S. Yan, W. Li, G. Alici, N.-T. Nguyen, *RSC Adv.* **2014**, *4*, 33149.
[8] Y. He, Z. Lu, K. Liu, L. Wang, Q. Xu, H. Fan, C. Liu, T. Zhang, *Sens. Actuators, B* **2024**, *399*, 134851.
[9] Y. Xiao, S. Li, Z. Pang, C. Wan, L. Li, H. Yuan, X. Hong, W. Du, X. Feng, Y. Li, *Biosens. Bioelectron.* **2022**, *206*, 114130.
[10] C. S. McGinnis, D. M. Patterson, J. Winkler, D. N. Conrad, M. Y. Hein, V. Srivastava, J. L. Hu, L. M. Murrow, J. S. Weissman, Z. Werb, *Nat. Methods* **2019**, *16*, 619.
[11] Y. Zhou, Y. Yang, D. Pappas, in *Microfluidic Chips for Sepsis Diagnosis*, Vol. *2321* (Ed. W. E. Walker), Humana, New York, NY **2021**, pp. 207–219.
[12] S. Cheng, Z. Wu, *Lab Chip* **2012**, *12*, 2782.
[13] H. H. Hansen, H. Cha, L. Ouyang, J. Zhang, B. Jin, H. Stratton, N.-T. Nguyen, H. An, *Biotechnol. Adv.* **2023**, *63*, 108091.
[14] S. Hettiarachchi, L. Ouyang, H. Cha, H. H. Hansen, H. An, N.-T. Nguyen, J. Zhang, *Nanoscale* **2024**, *16*, 3560.
[15] M. N. Islam, J. W. Yost, Z. R. Gagnon, *Analyst* **2022**, *147*, 587.
[16] K. Iwai, M. Wehrs, M. Garber, J. Sustarich, L. Washburn, Z. Costello, P. W. Kim, D. Ando, W. R. Gaillard, N. J. Hillson, *Microsyst. Nanoeng.* **2022**, *8*, 31.
[17] Y. Wu, M. Wu, A. Vázquez-Guardado, J. Kim, X. Zhang, R. Avila, J.-T. Kim, Y. Deng, Y. Yu, S. Melzer, *Nat. Commun.* **2022**, *13*, 5571.
[18] T. A. Duncombe, A. M. Tentori, A. E. Herr, *Nat. Rev. Mol. Cell Biol.* **2015**, *16*, 554.
[19] S. Regmi, C. Poudel, R. Adhikari, K. Q. Luo, *Biosensors* **2022**, *12*, 459.
[20] H. Fallahi, J. Zhang, H.-P. Phan, N.-T. Nguyen, *Micromachines* **2019**, *10*, 830.
[21] P. Simatos, L. Tian, R. Lindstedt, *Combust. Flame* **2022**, *239*, 111665.
[22] R. Absi, 8th International Conference on Fluid Mechanics (ICFM8), Tohoku, Japan, September **2018**.
[23] W. Mao, J. Xu, *Int. J. Heat Mass Transfer* **2009**, *52*, 5258.
[24] K. Ward, Z. H. Fan, *J. Micromech. Microeng.* **2015**, *25*, 094001.
[25] M. Asghari, X. Cao, B. Mateescu, D. Van Leeuwen, M. K. Aslan, S. Stavrakis, A. J. deMello, *ACS Nano* **2019**, *14*, 422.

[26] B. R. Mutlu, J. F. Edd, M. Toner, *Proc. Natl. Acad. Sci. USA* **2018**, *115*, 7682.
[27] M. Filippi, T. Buchner, O. Yasa, S. Weirich, R. K. Katzschmann, *Adv. Mater.* **2022**, *34*, 2108427.
[28] Q. Ma, H. Ma, F. Xu, X. Wang, W. Sun, *Microsyst. Nanoeng.* **2021**, *7*, 19.
[29] G. Valitov, D. Rossi, C. Price, A. Gavriilidis, L. Mazzei, *Chem. Eng. Process.* **2022**, *180*, 108629.
[30] T. Ma, S. Sun, B. Li, J. Chu, *Sens. Actuators, A* **2019**, *292*, 90.
[31] G. Vishwanathan, G. Juarez, *Microfluid. Nanofluid.* **2020**, *24*, 69.
[32] S. Lee, W. Lee, H. Kim, P. K. Bae, J. Park, J. Kim, *Biosens. Bioelectron.* **2019**, *131*, 280.
[33] I. Uvarov, S. Lemekhov, A. Melenev, V. Naumov, O. Koroleva, M. Izyumov, V. Svetovoy, *J. Phys.: Conf. Ser.* **2016**, *741*, 012167.
[34] S. Zhang, Y. Wang, R. Lavrijsen, P. R. Onck, J. M. den Toonder, *Sens. Actuators, B* **2018**, *263*, 614.
[35] S. Mi, H. Pu, S. Xia, W. Sun, *Sens. Actuators, A* **2020**, *301*, 111704.
[36] P.-H. Huang, N. Nama, Z. Mao, P. Li, J. Rufo, Y. Chen, Y. Xie, C.-H. Wei, L. Wang, T. J. Huang, *Lab Chip* **2014**, *14*, 4319.
[37] P. Marmottant, J. Raven, H. Gardeniers, J. Bomer, S. Hilgenfeldt, *J. Fluid Mech.* **2006**, *568*, 109.
[38] S. L. Truesdell, M. M. Saunders, *Microfluid. Nanofluid.* **2023**, *27*, 42.
[39] B. Mosadegh, C.-H. Kuo, Y.-C. Tung, Y.-S. Torisawa, T. Bersano-Begey, H. Tavana, S. Takayama, *Nat. Phys.* **2010**, *6*, 433.
[40] S.-J. Kim, R. Yokokawa, S. Cai Lesher-Perez, S. Takayama, *Nat. Commun.* **2015**, *6*, 7301.
[41] A. Saren, A. Smith, K. Ullakko, *Microfluid. Nanofluid.* **2018**, *22*, 38.
[42] P. Frank, J. Schreiter, S. Haefner, G. Paschew, A. Voigt, A. Richter, *PLoS One* **2016**, *11*, 0161024.
[43] J. Wu, Y. Hirai, K. I. Kamei, T. Tsuchiya, O. Tabata, *Electron. Commun. Jpn.* **2019**, *102*, 41.
[44] H. Xia, Z. Wang, W. Fan, A. Wijaya, W. Wang, Z. Wang, *Lab Chip* **2012**, *12*, 60.
[45] D. Cheng, Y. Yu, C. Han, M. Cao, G. Yang, J. Liu, X. Chen, Z. Peng, *Biomicrofluidics* **2018**, *12*, 34105.
[46] B. Dincau, E. Dressaire, A. Sauret, *Small* **2020**, *16*, 1904032.
[47] R. Absi, R. Azouani, *Proc. CIRP* **2018**, *78*, 359.
[48] K. S. Kim, M.-S. Chun, *Korea-Aust. Rheol. J.* **2012**, *24*, 89.
[49] S. Vedel, L. H. Olesen, H. Bruus, *J. Micromech. Microeng.* **2010**, *20*, 035026.
[50] S. M. Recktenwald, C. Wagner, T. John, *Lab Chip* **2021**, *21*, 2605.
[51] S. I. Abdelsalam, K. Vafai, *Math. Biosci.* **2017**, *283*, 91.
[52] M. Meki, A. El-Baz, P. Sethu, G. Giridharan, *Cells Tissues Organs* **2023**, *212*, 272.
[53] B. Dincau, C. Tang, E. Dressaire, A. Sauret, *Soft Matter* **2022**, *18*, 1767.
[54] J. White, M. Lancelot, S. Sarnaik, P. Hines, *Clin. Hemorheol. Microcirc.* **2015**, *60*, 201.
[55] Z. Chen, J. Zilberberg, W. Lee, *Biomed. Microdevices* **2020**, *22*, 58.
[56] J. Hwang, M. H. Ing, A. Salazar, B. Lassègue, K. Griendling, M. Navab, A. Sevanian, T. K. Hsiai, *Circ. Res.* **2003**, *93*, 1225.
[57] A. Malekanfard, S. Beladi-Behbahani, T.-R. Tzeng, H. Zhao, X. Xuan, *Anal. Chem.* **2021**, *93*, 5947.
[58] A. J. Moghadam, *Eur. J. Mech. -B/Fluids* **2021**, *85*, 158.
[59] H. Zhang, J. Yang, R. Sun, S. Han, Z. Yang, L. Teng, *Acta Pharm. Sin. B* **2023**, *13*, 3277.
[60] L. Capretto, D. Carugo, S. Mazzitelli, C. Nastruzzi, X. Zhang, *Adv. Drug Delivery Rev.* **2013**, *65*, 1496.
[61] N.-T. Nguyen, S. T. Wereley, S. A. M. Shaegh, *Fundamentals and Applications of Microfluidics*, 3rd ed., Artech house, London **2019**.
[62] K. W. Oh, K. Lee, B. Ahn, E. P. Furlani, *Lab Chip* **2012**, *12*, 515.
[63] M. Tikekar, S. G. Singh, A. Agrawal, *Microfluid. Nanofluid.* **2010**, *9*, 1225.
[64] P. Risch, D. Helmer, F. Kotz, B. E. Rapp, *Biosensors* **2019**, *9*, 67.
[65] A. Yakhot, M. Arad, G. Ben-Dor, *Int. J. Numer. Methods Fluids* **1999**, *29*, 935.
[66] L. Purtell, *Phys. Fluids* **1981**, *24*, 789.
[67] B. E. Rapp, in *Microfluidics: Modeling, Mechanics, and Mathematics*, 2nd ed., Elsevier, Amsterdam **2017**, pp. 303–308.
[68] J. Lee, A. Tripathi, A. Chauhan, *Chem. Eng. Sci.* **2014**, *117*, 183.
[69] H. Bruus, *Theoretical Microfluidics*, Oxford University Press, Oxford **2007**.
[70] Z. Li, C. Liu, J. Sun, *Lab Chip* **2023**, *23*, 3311.
[71] F. A. Perdigones, A. Luque, J. M. Quero, *IEEE Ind. Electron. Mag.* **2014**, *8*, 6.
[72] M. Karmozdi, H. Afshin, M. B. Shafii, *Sens. Actuators, A* **2020**, *301*, 111675.
[73] S. Battat, D. A. Weitz, G. M. Whitesides, *Chem. Rev.* **2022**, *122*, 6921.
[74] D. C. Leslie, C. J. Easley, E. Seker, J. M. Karlinsey, M. Utz, M. R. Begley, J. P. Landers, *Nat. Phys.* **2009**, *5*, 231.
[75] N.-T. Nguyen, *Mikrofluidik: Entwurf, Herstellung und Charakterisierung*, Springer-Verlag, Berlin **2013**.
[76] S. N. Makarov, R. Ludwig, S. J. Bitar, *Practical Electrical Engineering*, Springer, Cham **2019**, pp. 89–141.
[77] P. Skafte-Pedersen, M. Hemmingsen, D. Sabourin, F. S. Blaga, H. Bruus, M. Dufva, *Biomed. Microdevices* **2012**, *14*, 385.
[78] X. Y. Peng, L. Peng, Y. Guo, *Adv. Mater. Technol.* **2021**, *6*, 2100150.
[79] N. Rousset, C. Lohasz, J. A. Boos, P. M. Misun, F. Cardes, A. Hierlemann, *Micromachines* **2022**, *13*, 1124.
[80] K. A. Gopinathan, A. Mishra, B. R. Mutlu, J. F. Edd, M. Toner, *Nature* **2023**, *622*, 735.
[81] Y. Kim, B. Kuczenski, P. R. LeDuc, W. C. Messner, *Lab Chip* **2009**, *9*, 2603.
[82] M. R. Begley, M. Utz, D. C. Leslie, H. Haj-Hariri, J. Landers, H. Bart-Smith, *Appl. Phys. Lett.* **2009**, *95*, 203501.
[83] S.-J. Kim, R. Yokokawa, S. Takayama, *Appl. Phys. Lett.* **2012**, *101*, 234107.
[84] N. Xiang, Y. Han, Y. Jia, Z. Shi, H. Yi, Z. Ni, *Lab Chip* **2019**, *19*, 214.
[85] S. Södergren, K. Svensson, K. Hjort, *Sci. Rep.* **2021**, *11*, 22504.
[86] Y. Zhou, J. Liu, J. Yan, T. Zhu, S. Guo, S. Li, T. Li, *Micromachines* **2020**, *11*, 396.
[87] H. Xia, J. Wu, J. Zheng, J. Zhang, Z. Wang, *Lab Chip* **2021**, *21*, 1241.
[88] J. Lee, F. Rahman, T. Laoui, R. Karnik, *Phys. Rev. E* **2012**, *86*, 026301.
[89] M. Martí-Calatayud, M. Wessling, *J. Membr. Sci.* **2017**, *535*, 294.
[90] M. A. Sahin, M. Shehzad, G. Destgeer, *Small* **2023**, *20*, 2307956.
[91] A. Kalantarifard, E. A. Haghighi, C. Elbuken, *Chem. Eng. Sci.* **2018**, *178*, 238.
[92] M. A. Cartas Ayala, *Hydrodynamic Resistance and Sorting of Deformable Particles in Microfluidic Circuits*, Massachusetts Institute of Technology, Cambridge **2013**.
[93] P. Thurgood, J. Y. Zhu, N. Nguyen, S. Nahavandi, A. R. Jex, E. Pirogova, S. Baratchi, K. Khoshmanesh, *Lab Chip* **2018**, *18*, 2730.
[94] J. R. Lake, K. C. Heyde, W. C. Ruder, *PLoS One* **2017**, *12*, 0175089.
[95] L. Clime, J. Daoud, D. Brassard, L. Malic, M. Geissler, T. Veres, *Microfluid. Nanofluid.* **2019**, *23*, 29.
[96] R. Rimsa, A. Smith, C. Wälti, C. Wood, *Appl. Phys. Lett.* **2017**, *111*, 234102.
[97] P. K. Das, A. Hasan, *AIP Conf. Proc.* **2017**, *1851*, 020110.
[98] S. Mohith, P. N. Karanth, S. Kulkarni, *Mechatronics* **2019**, *60*, 34.
[99] C. Zhou, H. Zhang, Z. Li, W. Wang, *Lab Chip* **2016**, *16*, 1797.
[100] T. Tavari, M. Nazari, S. Meamardoost, A. Tamayol, M. Samandari, *Electrophoresis* **2022**, *43*, 1476.
[101] C. Wang, J. Park, *Micro Nano Syst. Lett.* **2020**, *8*, 1.
[102] A. Link, J. S. McGrath, M. Zaimagaoglu, T. Franke, *Lab Chip* **2022**, *22*, 193.
[103] B. Liu, C. Ma, J. Yang, D. Li, H. Liu, *Micromachines* **2021**, *12*, 1040.
[104] M. Li, Y. Su, H. Zhang, B. Dong, *Nano Res.* **2018**, *11*, 1810.

[105] P. De Stefano, E. Bianchi, G. Dubini, *Biomicrofluidics* **2022**, *16*, 031501.
[106] L. Xu, A. Wang, X. Li, K. W. Oh, *Biomicrofluidics* **2020**, *14*, 031503.
[107] G. Wang, H.-P. Ho, Q. Chen, A. K.-L. Yang, H.-C. Kwok, S.-Y. Wu, S.-K. Kong, Y.-W. Kwan, X. Zhang, *Lab Chip* **2013**, *13*, 3698.
[108] H. Zhang, R. D. Whalley, A. M. Ferreira, K. Dalgarno, *Prog. Biomed. Eng.* **2020**, *2*, 022001.
[109] Y. Chen, X. Chen, W. Lai, Q. Zhu, *AIP Adv.* **2022**, *12*, 105211.
[110] K. Khoshmanesh, A. Almansouri, H. Albloushi, P. Yi, R. Soffe, K. Kalantar-Zadeh, *Sci. Rep.* **2015**, *5*, 9942.
[111] J.-T. Yang, C.-K. Chen, K.-J. Tsai, W.-Z. Lin, H.-J. Sheen, *Sens. Actuators, A* **2007**, *135*, 476.
[112] E. Sweet, R. Mehta, Y. Xu, R. Jew, R. Lin, L. Lin, *Lab Chip* **2020**, *20*, 3375.
[113] P. Vazquez-Vergara, U. Torres-Herrera, G. A. Caballero-Robledo, L. F. Olguin, E. C. Poiré, *Front. Phys.* **2021**, *9*, 636070.
[114] T. Puttrich, S. O'Donnell, S.-W. Wong, M. Kotche, A. E. Felder, J.-W. Shin, *PLoS One* **2023**, *18*, 0282563.
[115] P. Ferretti, C. Pagliari, A. Montalti, A. Liverani, *Front. Mech. Eng.* **2023**, *9*, 1207464.
[116] C. Dietsche, B. R. Mutlu, J. F. Edd, P. Koumoutsakos, M. Toner, *Microfluid. Nanofluid.* **2019**, *23*, 83.
[117] Y. Wu, Y. Chen, Y. Cheng, *J. Chem. Educ.* **2024**, *101*, 1951.
[118] A. P. Iakovlev, A. S. Erofeev, P. V. Gorelkin, *Biosensors* **2022**, *12*, 956.
[119] C. K. Byun, K. Abi-Samra, Y. K. Cho, S. Takayama, *Electrophoresis* **2014**, *35*, 245.
[120] G. Eluru, J. V. Adhikari, P. Chanda, S. S. Gorthi, *Micromachines* **2020**, *11*, 67.
[121] J. X. Zhang, K. Hoshino, *Molecular Sensors and Nanodevices: Principles, Designs, and Applications in Biomedical Engineering*, Academic Press, Cambridge **2018**.
[122] D. W. Kim, D. J. Steward, *Pediatr. Anesth.* **1999**, *9*, 335.
[123] Y. J. Kang, *Phys. Fluids* **2023**, *35*, 121907.
[124] M. Weiss, T. Neff, A. Gerber, J. Fischer, *Pediatr. Anesth.* **2000**, *10*, 595.
[125] M. Hébert, W. Baxter, J. P. Huissoon, C. L. Ren, *Microfluid. Nanofluid.* **2020**, *24*, 90.
[126] J. I. Humadi, S. A. Gheni, S. M. Ahmed, G. H. Abdullah, A. N. Phan, A. P. Harvey, *Process Saf. Environ. Prot.* **2021**, *152*, 178.
[127] W. Zeng, S. Li, Z. Wang, presented at *2015 International Conference on Fluid Power and Mechatronics (FPM)*, Harbin, China, August **2015**.
[128] T. Glawdel, C. Elbuken, C. Ren, *Encycl. Microfluid. Nanofluid.* **2013**.
[129] H. Kim, D. Cheon, J. Lim, K. Nam, *IEEE Access* **2019**, *7*, 135427.
[130] L. M. Amarante, J. Newport, M. Mitchell, J. Wilson, M. Laubach, *eneuro* **2019**, *6*, ENEURO0240.
[131] M. Abolhasani, K. F. Jensen, *Lab Chip* **2016**, *16*, 2775.
[132] J. Prakash, D. Tripathi, *J. Mol. Liq.* **2018**, *256*, 352.
[133] I. Fatima, S. Asghar, *Adv. Mech. Eng.* **2020**, *12*, 168781402097106.
[134] M. R. Behrens, H. C. Fuller, E. R. Swist, J. Wu, M. M. Islam, Z. Long, W. C. Ruder, R. Steward Jr, *Sci. Rep.* **2020**, *10*, 1543.
[135] C. Koch, V. Remcho, J. Ingle, *Sens. Actuators, B* **2009**, *135*, 664.
[136] Y. Fung, C. Yih, *J. Appl. Mech.* **1968**, *35*, 669.
[137] M. Stork, D. Mayer, *IEEE Trans. Magn.* **2018**, *54*, 4600404.
[138] S. Wang, S. Li, M. Hu, B. Huo, *Biomicrofluidics* **2019**, *13*, 064117.
[139] W. Debrouwer, W. Kimpe, R. Dangreau, K. Huvaere, H. P. Gemoets, M. Mottaghi, S. Kuhn, K. Van Aken, *Org. Process Res. Dev.* **2020**, *24*, 2319.
[140] P. Skafte-Pedersen, D. Sabourin, M. Dufva, D. Snakenborg, *Lab Chip* **2009**, *9*, 3003.
[141] S. Hettiarachchi, G. Melroy, A. Mudugamuwa, N. Perera, P. Sampath, R. Amarasinghe, in *Sustainable Design and Manufacturing (KES-SDM 2021)*, *262*, (Eds: S. G. Scholz, R. J. Howlett, R. Setchi), Springer, Singapore **2022**, p. 235.
[142] J. Saunier, A. Khzam, N. Yagoubi, *J. Mech. Behav. Biomed. Mater.* **2022**, *136*, 105477.
[143] S. Schneider, M. Bubeck, J. Rogal, H. J. Weener, C. Rojas, M. Weiss, M. Heymann, A. D. van der Meer, P. Loskill, *Lab Chip* **2021**, *21*, 3963.
[144] E.-G. Kim, J.-g. Oh, B. Choi, *Sens. Actuators, A* **2006**, *128*, 43.
[145] N. Futai, W. Gu, J. W. Song, S. Takayama, *Lab Chip* **2006**, *6*, 149.
[146] T. Ching, J. Vasudevan, H. Y. Tan, C. T. Lim, J. Fernandez, Y.-C. Toh, M. Hashimoto, *HardwareX* **2021**, *10*, 00202.
[147] A. M. Nightingale, C. L. Leong, R. A. Burnish, S.-u. Hassan, Y. Zhang, G. F. Clough, M. G. Boutelle, D. Voegeli, X. Niu, *Nat. Commun.* **2019**, *10*, 2741.
[148] A. Banejad, S. A. M. Shaegh, E. Ramezani-Fard, P. Seifi, M. Passandideh-Fard, *Sens. Actuators, A* **2020**, *315*, 112242.
[149] M. Du, X. Ye, K. Wu, Z. Zhou, *Sensors* **2009**, *9*, 2611.
[150] M. Dehghan, M. Tahmasebipour, *Sens. Actuators, A* **2023**, *358*, 114431.
[151] J. Goulpeau, D. Trouchet, A. Ajdari, P. Tabeling, *J. Appl. Phys.* **2005**, *98*, 044914.
[152] T. Ma, Y. Wang, S. Sun, T. Pan, B. Li, J. Chu, *Sens. Actuators, A* **2022**, *334*, 113332.
[153] H. So, A. P. Pisano, Y. H. Seo, *Lab Chip* **2014**, *14*, 2240.
[154] W. Li, D. Li, L. He, Y. Wang, D. Wang, L. Qiao, *Rev. Sci. Instrum.* **2023**, *94*, 031502.
[155] G. R. Koirala, K. Shrestha, H. Lim, G. Cho, *Adv. Mater. Technol.* **2021**, *6*, 2001031.
[156] J. Xiang, Z. Cai, Y. Zhang, W. Wang, *Sens. Actuators, A* **2016**, *251*, 20.
[157] I. V. Uvarov, P. S. Shlepakov, A. E. Melenev, K. Ma, V. B. Svetovoy, G. J. Krijnen, *Actuators* **2021**, *10*, 62.
[158] K. Dradrach, M. Zmyślony, Z. Deng, A. Priimagi, J. Biggins, P. Wasylczyk, *Nat. Commun.* **2023**, *14*, 1877.
[159] F. Forouzandeh, A. Arevalo, A. Alfadhel, D. A. Borkholder, *Sens. Actuators, A* **2021**, *326*, 112602.
[160] F. Rahimi, S. Chatzimichail, A. Saifuddin, A. J. Surman, S. D. Taylor-Robinson, A. Salehi-Reyhani, *Chromatographia* **2020**, *83*, 1165.
[161] C.-D. Xue, J.-M. Zhao, Z.-P. Sun, J.-T. Na, Y.-J. Li, K.-R. Qin, *Microfluid. Nanofluid.* **2021**, *25*, 97.
[162] A. Dodge, E. Brunet, S. Chen, J. Goulpeau, V. Labas, J. Vinh, P. Tabeling, *Analyst* **2006**, *131*, 1122.
[163] B. R. Mutlu, T. Dubash, C. Dietsche, A. Mishra, A. Ozbey, K. Keim, J. F. Edd, D. A. Haber, S. Maheswaran, M. Toner, *Lab Chip* **2020**, *20*, 1612.
[164] P. Thurgood, S. Baratchi, A. Arash, E. Pirogova, A. R. Jex, K. Khoshmanesh, *Sci. Rep.* **2019**, *9*, 10600.
[165] P. Thurgood, S. A. Suarez, S. Chen, C. Gilliam, E. Pirogova, A. R. Jex, S. Baratchi, K. Khoshmanesh, *Lab Chip* **2019**, *19*, 2885.
[166] X. Luo, L. Yang, Y. Cui, *Sens. Actuators, A* **2023**, *363*, 114732.
[167] A. Alizadeh, W. L. Hsu, M. Wang, H. Daiguji, *Electrophoresis* **2021**, *42*, 834.
[168] Y. Takamura, H. Onoda, H. Inokuchi, S. Adachi, A. Oki, Y. Horiike, *Electrophoresis* **2003**, *24*, 185.
[169] M. Mehdipoor, R. H. Vafaie, A. Pourmand, E. Poorreza, H. B. Ghavifekr, presented at 8th International Symposium on Mechatronics and its Applications, Sharjah, UAE, April **2012**.
[170] Q. Yuan, K. Yang, J. Wu, *Microfluid. Nanofluid.* **2014**, *16*, 167.
[171] M. R. Hossan, D. Dutta, N. Islam, P. Dutta, *Electrophoresis* **2018**, *39*, 702.
[172] R. H. Vafaie, H. B. Ghavifekr, H. Van Lintel, J. Brugger, P. Renaud, *Electrophoresis* **2016**, *37*, 719.
[173] A. Nisar, N. Afzulpurkar, B. Mahaisavariya, A. Tuantranont, *Sens. Actuators, B* **2008**, *130*, 917.
[174] M. Stubbe, J. Gimsa, *Colloids Surf. A* **2011**, *376*, 97.
[175] R. Avila, C. Li, Y. Xue, J. A. Rogers, Y. Huang, *Proc. Natl. Acad. Sci. USA* **2021**, *118*, 2026405118.

[176] R. R. Gidde, P. M. Pawar, B. P. Ronge, V. P. Dhamgaye, *Microsyst. Technol.* **2019**, *25*, 509.
[177] H. Conrad, H. Schenk, B. Kaiser, S. Langa, M. Gaudet, K. Schimmanz, M. Stolz, M. Lenz, *Nat. Commun.* **2015**, *6*, 10078.
[178] S. Uhlig, M. Gaudet, S. Langa, K. Schimmanz, H. Conrad, B. Kaiser, H. Schenk, *Micromachines* **2018**, *9*, 190.
[179] C. Qi, N. Sugita, T. Shinshi, *Micromachines* **2022**, *13*, 1565.
[180] S. Dodampegama, A. Mudugamuwa, M. Konara, N. Perera, D. De Silva, U. Roshan, R. Amarasinghe, N. Jayaweera, H. Tamura, *Appl. Sci.* **2022**, *12*, 11542.
[181] J. Zhang, X. Ke, G. Gou, J. Seidel, B. Xiang, P. Yu, W.-I. Liang, A. M. Minor, Y.-H. Chu, G. Van Tendeloo, *Nat. Commun.* **2013**, *4*, 2768.
[182] U. Roshan, R. Amarasinghe, N. Dayananda, *J. Rob. Netw. Artif. Life* **2018**, *5*, 194.
[183] J. M. Robertson, R. Rodriguez, L. Holmes, P. Mather, E. Wetzel, *Smart Mater. Struct.* **2016**, *25*, 085043.
[184] J. Wu, H. Fang, J. Zhang, S. Yan, *J. Nanobiotechnol.* **2023**, *21*, 85.
[185] C. Qi, N. Sugita, T. Shinshi, presented at International Conference and Exhibition on New Actuator Systems and Applications, Mannheim, Germany, June **2022**.
[186] M. Z. Yildiz, H. A. Dereshgi, *J. Eng. Res.* **2019**, *7*, 226.
[187] W. Connacher, N. Zhang, A. Huang, J. Mei, S. Zhang, T. Gopesh, J. Friend, *Lab Chip* **2018**, *18*, 1952.
[188] H. Asadi Dereshgi, H. Dal, M. Z. Yildiz, *Microsyst. Technol.* **2021**, *27*, 4127.
[189] H. R. Hosseini, H. Nikookar, G. Yesiloz, M. Naseh, M. Mohammadi, *Adv. Bioenergy Microfluid. Appl.* **2021**, 365.
[190] Y. Guan, X. Meng, Y. Liu, M. Bai, F. Xu, *Int. J. Acoust. Vibr.* **2020**, *25*, 383.
[191] F. R. Munas, G. Melroy, C. B. Abeynayake, H. L. Chathuranga, R. Amarasinghe, P. Kumarage, V. T. Dau, D. V. Dao, *Sensors* **2018**, *18*, 1302.
[192] S. A. F. Farshchi Yazdi, A. Corigliano, R. Ardito, *Micromachines* **2019**, *10*, 259.
[193] Z. Wu, H. Cai, Z. Ao, A. Nunez, H. Liu, M. Bondesson, S. Guo, F. Guo, *Anal. Chem.* **2019**, *91*, 7097.
[194] H. Bachman, P.-H. Huang, S. Zhao, S. Yang, P. Zhang, H. Fu, T. J. Huang, *Lab Chip* **2018**, *18*, 433.
[195] Y. Gao, M. Wu, Y. Lin, W. Zhao, J. Xu, *Microfluid. Nanofluid.* **2020**, *24*, 29.
[196] P. Thurgood, G. Concilia, N. Tran, N. Nguyen, A. J. Hawke, E. Pirogova, A. R. Jex, K. Peter, S. Baratchi, K. Khoshmanesh, *Lab Chip* **2021**, *21*, 4672.
[197] Z. Tang, X. Shao, J. Huang, J. Yao, G. Ding, *Nanotechnol. Precis. Eng. (NPE)* **2019**, *2*, 95.
[198] C. Eilenberger, M. Rothbauer, F. Selinger, A. Gerhartl, C. Jordan, M. Harasek, B. Schädl, J. Grillari, J. Weghuber, W. Neuhaus, *Adv. Sci.* **2021**, *8*, 2004856.
[199] P. A. Basilio, A. M. Torres Rojas, E. Corvera Poiré, L. F. Olguín, *Microfluid. Nanofluid.* **2019**, *23*, 64.
[200] M. Saito, Y. Kasai, H. Kumon, S. Sakuma, F. Arai, presented at 2020 IEEE 33rd International Conference on Micro Electro Mechanical Systems (MEMS), Vancouver, BC, Canada, January **2020**.
[201] J. Dong, Y. Cao, Q. Chen, Y. Wu, R. G. Liu, W. Liu, Y. Yang, Z. Yang, *J. Intell. Mater. Syst. Struct.* **2020**, *31*, 117.
[202] F. Zhao, X. Chen, J. Zhang, X. Zhang, J. Xie, L. Jin, Z. Liu, J. Zhuang, W. Ren, Z. G. Ye, *Sens. Actuators, B* **2021**, *347*, 130611.
[203] N. Ota, Y. Yalikun, T. Suzuki, S. W. Lee, Y. Hosokawa, K. Goda, Y. Tanaka, *R. Soc. Open Sci.* **2019**, *6*, 181776.
[204] J. Rufo, F. Cai, J. Friend, M. Wiklund, T. J. Huang, *Nat. Rev. Methods Primers* **2022**, *2*, 30.
[205] P. N. Amaniampong, Q. T. Trinh, T. Bahry, J. Zhang, F. Jérôme, *Green Chem.* **2022**, *24*, 4800.
[206] Y. Fan, X. Wang, J. Ren, F. Lin, J. Wu, *Microsyst. Nanoeng.* **2022**, *8*, 94.
[207] Y. Lin, Y. Gao, M. Wu, R. Zhou, D. Chung, G. Caraveo, J. Xu, *Lab Chip* **2019**, *19*, 3045.
[208] F. Akkoyun, A. Özçelik, *Actuators* **2022**, *11*, 116.
[209] Y.-T. Kao, T. S. Kaminski, W. Postek, J. Guzowski, K. Makuch, A. Ruszczak, F. von Stetten, R. Zengerle, P. Garstecki, *Lab Chip* **2020**, *20*, 54.
[210] K. R. Bajgiran, A. S. Cordova, R. Elkhanoufi, J. A. Dorman, A. T. Melvin, *Micromachines* **2021**, *12*, 1211.
[211] A. Petrosyan, P. Cravedi, V. Villani, A. Angeletti, J. Manrique, A. Renieri, R. E. De Filippo, L. Perin, S. Da Sacco, *Nat. Commun.* **2019**, *10*, 3656.
[212] H. Zhang, W. Duan, M. Lu, X. Zhao, S. Shklyaev, L. Liu, T. J. Huang, A. Sen, *ACS Nano* **2014**, *8*, 8537.
[213] L. Xu, F. Mou, H. Gong, M. Luo, J. Guan, *Chem. Soc. Rev.* **2017**, *46*, 6905.
[214] A. Mudugamuwa, S. Hettiarachchi, G. Melroy, S. Dodampegama, M. Konara, U. Roshan, R. Amarasinghe, D. Jayathilaka, P. Wang, *Sensors* **2022**, *22*, 6900.
[215] B. Van Dang, S.-J. Kim, *Lab Chip* **2017**, *17*, 286.
[216] H. Xia, Z. Wang, W. Wang, W. Fan, A. Wijaya, Z. Wang, *Lab Chip* **2013**, *13*, 1619.
[217] M. Cheikh, I. Lakkis, *Microfluid. Nanofluid.* **2016**, *20*, 91.
[218] G. Weisgrab, A. Ovsianikov, P. F. Costa, *Adv. Mater. Technol.* **2019**, *4*, 1900275.
[219] R. Greiner, M. Allerdissen, A. Voigt, A. Richter, *Lab Chip* **2012**, *12*, 5034.
[220] P. Frank, D. Gräfe, C. Probst, S. Haefner, M. Elstner, D. Appelhans, D. Kohlheyer, B. Voit, A. Richter, *Adv. Funct. Mater.* **2017**, *27*, 1700430.
[221] A. Beck, P. J. Mehner, A. Voigt, F. Obst, U. Marschner, A. Richter, *Adv. Mater. Technol.* **2022**, *7*, 2200185.
[222] Q. Zhang, M. Zhang, L. Djeghlaf, J. Bataille, J. Gamby, A. M. Haghiri-Gosnet, A. Pallandre, *Electrophoresis* **2017**, *38*, 953.
[223] S.-J. Kim, R. Yokokawa, S. Takayama, *Lab Chip* **2013**, *13*, 1644.
[224] S.-J. Kim, R. Yokokawa, S. C. Lesher-Perez, S. Takayama, *Anal. Chem.* **2012**, *84*, 1152.
[225] G. Kim, B. Van Dang, S.-J. Kim, *Sens. Actuators, B* **2018**, *266*, 614.
[226] J.-Y. Qian, C.-W. Hou, X.-J. Li, Z.-J. Jin, *Micromachines* **2020**, *11*, 172.
[227] A. Gholizadeh, S. Abbaslou, P. Xie, A. Knaian, M. Javanmard, *Sens. Actuators, A* **2019**, *296*, 316.
[228] J.-M. Zhao, Y.-F. Yin, J. Liu, Y.-J. Li, Y. Wang, C.-D. Xue, K.-R. Qin, *Sens. Actuators, A* **2023**, *359*, 114505.
[229] A. Beck, F. Obst, D. Gruner, A. Voigt, P. J. Mehner, S. Gruenzner, R. Koerbitz, M. H. Shahadha, A. Kutscher, G. Paschew, *Adv. Mater. Technol.* **2023**, *8*, 2200417.
[230] Y. Aishan, Y. Yalikun, Y. Shen, Y. Yuan, S. Amaya, T. Okutaki, A. Osaki, S. Maeda, Y. Tanaka, *Sens. Actuators, B* **2021**, *337*, 129769.
[231] G. Paschew, J. Schreiter, A. Voigt, C. Pini, J. P. Chávez, M. Allerdißen, U. Marschner, S. Siegmund, R. Schüffny, F. Jülicher, *Adv. Mater. Technol.* **2016**, *1*, 1600005.
[232] M. M. Sadeghi, H. S. Kim, R. L. B. Peterson, K. Najafi, *J. Microelectromech. Syst.* **2016**, *25*, 557.
[233] T. Thalhofer, M. Keck, S. Kibler, O. Hayden, *Sensors* **2022**, *22*, 1273.
[234] S.-S. Li, C.-M. Cheng, *Lab Chip* **2013**, *13*, 3782.
[235] Y. Ma, M. Sun, X. Duan, A. van den Berg, J. C. Eijkel, Y. Xie, *Nat. Commun.* **2020**, *11*, 814.
[236] H. Xia, J. Wu, Z. Wang, *J. Micromech. Microeng.* **2017**, *27*, 075001.
[237] Y. Xie, C. Chindam, N. Nama, S. Yang, M. Lu, Y. Zhao, J. D. Mai, F. Costanzo, T. J. Huang, *Sci. Rep.* **2015**, *5*, 12572.
[238] F. R. Phelan, P. Kutty, J. A. Pathak, *Microfluid. Nanofluid.* **2008**, *5*, 101.
[239] A. Bertsch, A. Bongarzone, M. Duchamp, P. Renaud, F. Gallaire, *Phys. Rev. Fluids* **2020**, *5*, 054202.
[240] B. Rallabandi, C. Wang, S. Hilgenfeldt, *Phys. Rev. Fluids* **2017**, *2*, 064501.

[241] X. Wang, X. Chen, X. Ma, X. Kong, Z. Xu, J. Wang, *Talanta* **2011**, *84*, 565.
[242] P. Zhu, X. Tang, Y. Tian, L. Wang, *Sci. Rep.* **2016**, *6*, 31436.
[243] A. M. Guzmán, M. P. Beiza, A. J. Diaz, P. F. Fischer, J. C. Ramos, *Int. J. Heat Mass Transfer* **2013**, *58*, 568.
[244] M. Ghafarian, D. Mohebbi-Kalhori, J. Sadegi, *Int. J. Thermal Sci.* **2013**, *66*, 42.
[245] T. E. Walsh, K. Yang, V. Nee, Q. Liao, in *Experimental Heat Transfer, Fluid Mechanics and Thermodynamics*, Elsevier, Amsterdam **1993**, pp. 641–648.
[246] L. Liang, X. Wang, D. Chen, P. Sethu, G. A. Giridharan, Y. Wang, Y. Wang, K.-R. Qin, *Lab Chip* **2024**, *24*, 2428.
[247] D. Benzinger, M. Khammash, *Nat. Commun.* **2018**, *9*, 3521.
[248] A.-N. Cho, Y. Jin, Y. An, J. Kim, Y. S. Choi, J. S. Lee, J. Kim, W.-Y. Choi, D.-J. Koo, W. Yu, *Nat. Commun.* **2021**, *12*, 4730.
[249] W. M. Abed, R. D. Whalley, D. J. Dennis, R. J. Poole, *J. Non-Newtonian Fluid Mech.* **2016**, *231*, 68.
[250] I. A. Loe, T. Zheng, K. Kotani, Y. Jimbo, *Sci. Rep.* **2023**, *13*, 8852.
[251] J. Wu, H. Xia, Y. Zhang, S. Zhao, P. Zhu, Z. Wang, *Microsyst. Technol.* **2019**, *25*, 2741.
[252] H. M. Hmood, S. A. Gheni, S. M. Ahmed, M. M. Ali, H. Y. Saleh, M. H. Mohammed, A. E. Mohammed, M. A. Mahomood, H. R. Mohammed, A. A. Hassan, *Particuology* **2024**, *84*, 249.
[253] I. A. Loe, H. Nakao, Y. Jimbo, K. Kotani, *J. Fluid Mech.* **2021**, *911*, R2.
[254] M. Wang, G. Liu, R. Liu, Y. Feng, X. Li, C. Wang, X. Sun, *Measurement* **2024**, *227*, 114277.
[255] R. Van Erp, R. Soleimanzadeh, L. Nela, G. Kampitsis, E. Matioli, *Nature* **2020**, *585*, 211.
[256] Y. Zhang, H. Xia, *Sens. Actuators, B* **2022**, *368*, 132183.
[257] A. Tripathi, H. Shum, A. C. Balazs, *Soft Matter* **2014**, *10*, 1416.
[258] S. M. McFaul, B. K. Lin, H. Ma, *Lab Chip* **2012**, *12*, 2369.
[259] J. Shi, P. Zhu, J. Liu, R. Shen, H. Xia, H. Jiang, S. Xu, F. Zhao, *Ind. Eng. Chem. Res.* **2022**, *61*, 17593.
[260] G. D. Priyadarsini, G. Sankad, *Phys. Fluids* **2023**, *35*, 112001.
[261] J. Qu, H. Wu, P. Cheng, Q. Wang, Q. Sun, *Int. J. Heat Mass Transfer* **2017**, *110*, 294.
[262] H. Yang, G. Yao, D. Wen, *Exp. Therm. Fluid Sci.* **2020**, *112*, 109997.
[263] W. M. Abed, R. D. Whalley, D. J. Dennis, R. J. Poole, *Int. J. Heat Mass Transfer* **2015**, *88*, 790.
[264] R. Whalley, W. Abed, D. Dennis, R. Poole, *Theor. Appl. Mech. Lett.* **2015**, *5*, 103.
[265] J. Choi, Y. Zhang, *Numer. Heat Transfer, Part A: Appl.* **2020**, *77*, 761.
[266] E. Y. Basova, F. Foret, *Analyst* **2015**, *140*, 22.
[267] H. Liu, M. Li, Y. Wang, J. Piper, L. Jiang, *Micromachines* **2020**, *11*, 94.
[268] E. Brouzes, M. Medkova, N. Savenelli, D. Marran, M. Twardowski, J. B. Hutchison, J. M. Rothberg, D. R. Link, N. Perrimon, M. L. Samuels, *Proc. Natl. Acad. Sci. USA* **2009**, *106*, 14195.
[269] L. Mazutis, J. Gilbert, W. L. Ung, D. A. Weitz, A. D. Griffiths, J. A. Heyman, *Nat. Protoc.* **2013**, *8*, 870.
[270] H. N. Joensson, H. A. Svahn, *Angew. Chem., Int. Ed.* **2012**, *51*, 12176.
[271] J. Nunes, S. Tsai, J. Wan, H. A. Stone, *J. Phys. D: Appl. Phys.* **2013**, *46*, 114002.
[272] A. Dewandre, J. Rivero-Rodriguez, Y. Vitry, B. Sobac, B. Scheid, *Sci. Rep.* **2020**, *10*, 21616.
[273] P. Zhu, L. Wang, *Lab Chip* **2017**, *17*, 34.
[274] Y. Song, D. Cheng, L. Zhao, *Microfluidics: Fundamentals, Devices, and Applications*, John Wiley & Sons, Hoboken, NJ **2018**.
[275] Y. Zhang, H. Xia, J. Wu, J. Zhang, Z. Wang, *Appl. Phys. Lett.* **2019**, *114*, 073701.
[276] M. Wang, H. Xia, L. Zhu, *Ind. Eng. Chem. Res.* **2024**, *63*, 2432.
[277] A. Sauret, C. Spandagos, H. C. Shum, *Lab Chip* **2012**, *12*, 3380.
[278] I. Ziemecka, V. van Steijn, G. J. Koper, M. Rosso, A. M. Brizard, J. H. van Esch, M. T. Kreutzer, *Lab Chip* **2011**, *11*, 620.
[279] A. Sauret, H. Cheung Shum, *Appl. Phys. Lett.* **2012**, *100*, 154106.
[280] Y. Zhang, J. Zhang, Z. Tang, Q. Wu, *Chem. Eng. J.* **2021**, *417*, 129055.
[281] M. Wang, H. Xia, L. Zhu, Y. Zhang, *Ind. Eng. Chem. Res.* **2023**, *62*, 1997.
[282] Y. Wu, Y. Meng, *TrAC Trends Anal. Chem.* **2023**, *168*, 117301.
[283] S. Hettiarachchi, H. Cha, L. Ouyang, A. Mudugamuwa, H. An, G. Kijanka, N. Kashaninejad, N.-T. Nguyen, J. Zhang, *Lab Chip* **2023**, *23*, 982.
[284] H. Cha, H. Fallahi, Y. Dai, D. Yuan, H. An, N.-T. Nguyen, J. Zhang, *Lab Chip* **2022**, *22*, 423.
[285] B. Cetin, M. B. Özer, M. E. Solmaz, *Biochem. Eng. J.* **2014**, *92*, 63.
[286] S. Zhang, Y. Wang, P. Onck, J. den Toonder, *Microfluid. Nanofluid.* **2020**, *24*, 24.
[287] Z. Lu, E. D. Dupuis, V. K. Patel, A. M. Momen, S. Shahab, *Phys. Fluids* **2021**, *33*, 032003.
[288] M. Sun, K. Han, R. Hu, D. Liu, W. Fu, W. Liu, *Adv. Healthcare Mater.* **2021**, *10*, 2001545.
[289] M. Sharma, S. Remanan, G. Madras, S. Bose, *Ind. Eng. Chem. Res.* **2017**, *56*, 2025.
[290] Y. Cheng, Y. Wang, Z. Ma, W. Wang, X. Ye, *Lab Chip* **2016**, *16*, 4517.
[291] V. V. Ryzhkov, A. V. Zverev, V. V. Echeistov, M. Andronic, I. A. Ryzhikov, I. A. Budashov, A. V. Eremenko, I. N. Kurochkin, I. A. Rodionov, *Sci. Rep.* **2020**, *10*, 21107.
[292] D. Venugopal, N. Kasani, Y. Manjunath, G. Li, J. T. Kaifi, J. W. Kwon, *Sci. Rep.* **2021**, *11*, 16685.
[293] J. Howell, R. Field, D. Wu, *J. Membr. Sci.* **1993**, *80*, 59.
[294] B. Olayiwola, P. Walzel, *J. Membr. Sci.* **2009**, *345*, 36.
[295] J. Wang, Q. Jin, Y. Zhang, H. Fang, H. Xia, *Sep. Purif. Technol.* **2021**, *272*, 118854.
[296] Z. Li, C. Liu, Y. Cheng, Y. Li, J. Deng, L. Bai, L. Qin, H. Mei, M. Zeng, F. Tian, *Sci. Adv.* **2023**, *9*, ade2819.
[297] G. Lestari, A. Salari, M. Abolhasani, E. Kumacheva, *Lab Chip* **2016**, *16*, 2710.
[298] C. M. Leung, P. De Haan, K. Ronaldson-Bouchard, G.-A. Kim, J. Ko, H. S. Rho, Z. Chen, P. Habibovic, N. L. Jeon, S. Takayama, *Nat. Rev. Methods Primers* **2022**, *2*, 33.
[299] K. Cameron, M. El Hassan, R. Sabbagh, D. H. Freed, D. S. Nobes, *PLoS One* **2020**, *15*, 0239604.
[300] D. Zhalmuratova, T.-G. La, K. T.-T. Yu, A. R. Szojka, S. H. Andrews, A. B. Adesida, C.-I. Kim, D. S. Nobes, D. H. Freed, H.-J. Chung, *ACS Appl. Mater. Interfaces* **2019**, *11*, 33323.
[301] A. Selahi, S. Chakraborty, M. Muthuchamy, D. C. Zawieja, A. Jain, *Analyst* **2022**, *147*, 2953.
[302] C. Yang, W. Li, Y. Zhao, L. Shang, *Proc. Natl. Acad. Sci. USA* **2024**, *121*, 2402331121.
[303] C. Yang, Y. Yu, L. Shang, Y. Zhao, *Nat. Chem. Eng.* **2024**, *1*, 87.
[304] R. Kedarasetti, P. Drew, F. Costanzo, *Sci. Rep.* **2020**, *10*, 10102.
[305] J. Li, O. Lao, R. E. Nordon, *MethodsX* **2021**, *8*, 101269.
[306] N. Jen, J. Hadfield, G. M. Bessa, M. Amabili, D. S. Nobes, H.-J. Chung, *J. Mech. Behav. Biomed. Mater.* **2023**, *145*, 105994.
[307] N. Jen, G. M. Bessa, K. Nicolson, J. Xiao, D. S. Nobes, H.-J. Chung, *Iscience* **2022**, *25*, 104369.
[308] J. E. Moore Jr, C. D. Bertram, *Annu. Rev. Fluid Mech.* **2018**, *50*, 459.
[309] G. Miserocchi, *Eur. Respir. J.* **1997**, *10*, 219.
[310] A. Selahi, T. Fernando, S. Chakraborty, M. Muthuchamy, D. C. Zawieja, A. Jain, *Lab Chip* **2022**, *22*, 121.
[311] H. A. Barnes, J. F. Hutton, K. Walters, *An Introduction to Rheology*, Elsevier, Amsterdam **1989**.
[312] H. Rahmani, F. Larachi, S. M. Taghavi, *ACS Eng. Au* **2024**, *4*, 166.
[313] L. Casanellas, M. A. Alves, R. J. Poole, S. Lerouge, A. Lindner, *Soft Matter* **2016**, *12*, 6167.
[314] D. C. Vadillo, W. Mathues, C. Clasen, *Rheol. Acta* **2012**, *51*, 755.
[315] A. M. Torres Rojas, E. C. Poiré, *Phys. Rev. Fluids* **2020**, *5*, 063303.
[316] F. Del Giudice, S. J. Haward, A. Q. Shen, *J. Rheol.* **2017**, *61*, 327.

[317] C. Trejo-Soto, G. R. Lázaro, I. Pagonabarraga, A. Hernández-Machado, *Membranes* **2022**, *12*, 217.
[318] D. Tammaro, G. D'Avino, S. Costanzo, E. Di Maio, N. Grizzuti, P. L. Maffettone, *Polym. Test.* **2021**, *102*, 107332.
[319] B. Ismail, I. Haffar, R. Baalbaki, Y. Mechref, J. Henry, *Int. J. Food Sci. Technol.* **2006**, *41*, 919.
[320] A. Tarafdar, B. P. Kaur, P. K. Nema, O. A. Babar, D. Kumar, *Lwt* **2020**, *123*, 109058.
[321] P. Cicuta, A. M. Donald, *Soft Matter* **2007**, *3*, 1449.
[322] V. Sharma, A. Jaishankar, Y.-C. Wang, G. H. McKinley, *Soft Matter* **2011**, *7*, 5150.
[323] F. Del Giudice, *Phys. Fluids* **2020**, *32*, 052001.
[324] Y. Zhou, C. M. Schroeder, *Macromolecules* **2016**, *49*, 8018.
[325] F. Del Giudice, *Micromachines* **2022**, *13*, 167.
[326] J. Odell, S. Carrington, *J. Non-Newtonian Fluid Mech.* **2006**, *137*, 110.
[327] J. D. Park, S. A. Rogers, *Phys. Fluids* **2020**, *32*, 063102.
[328] R. van Buel, H. Stark, *Sci. Rep.* **2020**, *10*, 15704.
[329] M. Andersson, M. Karlsson, *Biomech. Model. Mechanobiol* **2021**, *20*, 491.
[330] S. Gupta, C. Sasmal, *Phys. Fluids* **2023**, *35*, 033114.
[331] A. Brambila-Solórzano, F. Méndez-Lavielle, J. L. Naude, G. J. Martínez-Sánchez, A. García-Rebolledo, B. Hernández, C. Escobar-del Pozo, *Bioengineering* **2023**, *10*, 1170.
[332] F. Wang, C. Pan, Q. Tian, B. Hua, *J. Micromech. Microeng.* **2023**, *33*, 045002.
[333] M. Wang, J. Xu, W. Ren, Z. Yang, *Nanomanuf. Metrol.* **2024**, *7*, 15.
[334] W. Ren, J. Xu, Z. Lian, X. Sun, Z. Xu, H. Yu, *Int. J. Extreme Manuf.* **2021**, *4*, 015101.
[335] C. Yang, Y. Yu, X. Wang, L. Shang, Y. Zhao, *Small* **2022**, *18*, 2104309.
[336] S.-Y. Tang, K. Khoshmanesh, V. Sivan, P. Petersen, A. P. O'Mullane, D. Abbott, A. Mitchell, K. Kalantar-Zadeh, *Proc. Natl. Acad. Sci. USA* **2014**, *111*, 3304.
[337] M. Urso, L. Bruno, S. Dattilo, S. C. Carroccio, S. Mirabella, *ACS Appl. Mater. Interfaces* **2023**, *16*, 1293.
[338] M. Ikram, F. Hu, G. Peng, M. Basharat, N. Jabeen, K. Pan, Y. Gao, *ACS Appl. Mater. Interfaces* **2021**, *13*, 51799.
[339] S. O'Halloran, A. Pandit, A. Heise, A. Kellett, *Adv. Sci.* **2023**, *10*, 2204072.
[340] M. Carlotti, V. Mattoli, *Small* **2019**, *15*, 1902687.
[341] S. Maruo, H. Inoue, *Appl. Phys. Lett.* **2006**, *89*, 144101.
[342] C. Zheng, F. Jin, Y. Zhao, M. Zheng, J. Liu, X. Dong, Z. Xiong, Y. Xia, X. Duan, *Sens. Actuators, B* **2020**, *304*, 127345.
[343] N.-T. Nguyen, *Micromachines* **2020**, *11*, 1004.
[344] U. Roshan, A. Mudugamuwa, H. Cha, S. Hettiarachchi, J. Zhang, N.-T. Nguyen, *Lab Chip* **2024**, *24*, 2146.
[345] H. M. Musharaf, U. Roshan, A. Mudugamuwa, Q. T. Trinh, J. Zhang, N.-T. Nguyen, *Micromachines* **2024**, *15*, 897.
[346] G. Gonzalez, I. Roppolo, C. F. Pirri, A. Chiappone, *Addit. Manuf.* **2022**, *55*, 102867.

Amith Mudugamuwa received his Bachelor's degree in mechanical engineering from the University of Moratuwa (UOM), Sri Lanka in 2017. He received his M.Phil. in mechatronic engineering from Shandong University of Science and Technology (SDUST), China in 2020. At present, he is a Ph.D. candidate at Queensland Micro- and Nanotechnology Centre (QMNC), Griffith University, Australia. His current research focuses on innovative inertial microfluidics for micro/nano particle manipulation. His research interests include microfluidics, lab-on-a-chip, acoustofluidics, micro/nano-electromechanical systems (MEMS/NEMS), machine vision, vibration-based sensing, and artificial intelligence.

Uditha Roshan received his Bachelor of the Science of Engineering Honours and the M.Phil. degrees in mechanical engineering from the University of Moratuwa, Sri Lanka in 2016 and 2022 respectively. He started his doctoral studies in 2023 and is currently a Ph.D. candidate at Queensland Micro- and Nanotechnology Centre (QMNC), Griffith University, Australia. His research focuses on design and development of microelastofluidic systems for biomedical applications. His research interests are microfluidics, microelastofluidics, smart material-based actuation, and micro/nano-electromechanical systems (MEMS/NEMS).

Nam-Trung Nguyen is an Australian Laureate Fellow. He received his Dipl-Ing, Dr Ing, and Dr Ing Habil degrees from Chemnitz University of Technology, Germany, in 1993, 1997, and 2004, respectively. From 1999 to 2013, he was an associate professor at Nanyang Technological University in Singapore. Since 2013, he has served as a professor and the Director of Queensland Micro- and Nanotechnology Centre of Griffith University, Australia. He is a fellow of ASME and a senior member of IEEE. His research is focused on microfluidics, nanofluidics, micro/nanomachining technologies, micro/nanoscale science, and instrumentation for biomedical applications. One of his current research interests is developing flexible and stretchable systems with bio interface.

Jun Zhang is a senior lecturer at the School of Engineering and Built Environment, Griffith University, Australia. He is a recipient of an ARC DECRA (2021-23) and Future (2025-2029) fellowships. He received his Bachelor's degree in engineering with an Outstanding Graduate Award from the Nanjing University of Science and Technology (NUST), China, in 2009, and received a Ph.D. degree in mechanical engineering from the University of Wollongong, Australia, in 2015. His research is to explore the passive fluid dynamics, active external (electrical, acoustic, magnetic etc.) force fields and their combination to accurately manipulate micro- and nanoparticles in rigid and flexible microfluidic platforms, as well as develop microfluidic technologies for disease diagnosis and therapeutics.